*Revision, changes marked

Opening of a trans-Pangaean marine corridor during the Early Jurassic: Insights from osmium isotopes across the Sinemurian–Pliensbachian GSSP, Robin Hood's Bay, UK.

Sarah J. Porter [a, *], David Selby [a], Katsuhiko Suzuki [b], Darren Gröcke [a]

[a] *Department of Earth Sciences, Durham University, Durham, DH1 3LE, UK.*
[b] *Japan-Agency for Marine-Earth Science and Technology, Yokosuka, 237-0061, Japan.*
[*] *Corresponding author (S. J. Porter). Tel.: +44 (0)191 334 2300; fax: +44 (0191) 334 2301; E-mail: sporter@eos.ubc.ca*

Keywords: Osmium isotopes, Hispanic Corridor, Sinemurian–Pliensbachian, organic-rich sediments, ocean connectivity

ABSTRACT

The Hispanic Corridor represents a significant phase of continental reorganisation of the Early Jurassic that eventually provided connectivity between the western Tethyan and eastern Pacific oceans along the Central Atlantic rift zone. Although the initiation of this marine corridor profoundly impacted oceanic circulation and marine faunal exchange patterns, the timing of its formation hitherto remains poorly constrained with estimates spanning both the Hettangian and Sinemurian. The Sinemurian–Pliensbachian Global Stratotype Section and Point (GSSP) at Robin Hood's Bay, UK, comprises a succession of well-exposed, immature organic-rich sediments, only previously characterised by strontium, oxygen and carbon isotope geochemistry. New Re and Os isotope profiling indicates substantial variation in seawater chemistry at this time. Initial osmium isotope data become increasing unradiogenic (0.40 to 0.20) across the boundary, providing evidence for a continual flux of unradiogenic Os into the oceans during the latest Sinemurian. The initial unradiogenic $^{187}Os/^{188}Os$ values indicate the occurrence of low-temperature hydrothermal activity associated with the formation of the Hispanic Corridor during the breakup of Pangaea. Therefore, combined with biogeography and faunal exchange patterns, the Os isotope data demonstrates that connectivity between the Eastern Pacific and Tethyan oceans initiated during the latest Sinemurian.

As a result this study better constrains the timing of establishment of the Hispanic Corridor, which was previously limited to poorly defined biogeography.

1. Introduction

Marine sedimentary rocks hold the key to understanding past chemical changes and fluxes in the oceans. Analysis of hydrogenous rhenium (Re) and osmium (Os) in organic-rich sediments allows detailed evaluation of seawater chemistry at the time of sediment deposition. The Os isotope system ($^{187}Os/^{188}Os$) is a particularly powerful tool for tracing temporal changes in the balance of global inputs to the oceans (Ravizza et al., 1996; Levasseur et al., 1999; Cohen et al., 1999; Peucker-Ehrenbrink and Ravizza, 2000), and as such it permits the evaluation of fluctuations in seawater chemistry throughout geological time. Specifically, significant input from meteorite impact, continental weathering and mantle-derived fluxes can be identified and distinguished.

The present-day seawater Os isotope composition may be relatively uniform ($^{187}Os/^{188}Os$ ratio of ~1.06; Levasseur et al., 1998; Peucker-Ehrenbrink and Ravizza, 2000), but it has varied significantly throughout geological time. The short seawater residence time of Os of ~10–40 Ka (Sharma et al., 1997; Oxburgh, 1998; Levasseur et al., 1998; Peucker-Ehrenbrink and Ravizza, 2000), longer than the mixing time of the oceans (~2–4 Ka; Palmer et al., 1988), allows the Os isotope composition to respond rapidly to any alterations in the composition and flux of these inputs (Oxburgh, 1998; Cohen et al., 1999). This has been successfully exploited by past studies, where Os has been used as a chemostratigraphic marker of significant volcanic events (eg., Cohen et al., 1999; Ravizza and Peucker-Ehrenbrink, 2003).

Until now, isotope stratigraphy of the Sinemurian–Pliensbachian GSSP at Robin Hood's Bay (Wine Haven, UK) has been limited to $^{87}Sr/^{86}Sr$ (Jones et al., 1994; Hesselbo et al., 2000), $\delta^{18}O$ and $\delta^{13}C$ data (Hesselbo et al., 2000) from belemnites. Herein we compile these datasets with Re-Os data, to provide new Os isotope characterisation of the Sinemurian–Pliensbachian GSSP. The longer

seawater residence time of Sr (~2.4 Ma; Jones and Jenkyns, 2001) relative to Os, slows the response of Sr ratios to changes in the balances of inputs to the oceans (eg. Cohen and Coe, 2002). Therefore, using Os isotopes provides improved resolution for changes in seawater chemistry across this boundary section. Combined with data from previous studies this work has two significant outcomes, by providing: (1) an increased geochemical understanding of an important GSSP, thereby also enhancing our understanding of Lower Jurassic stratigraphy in the UK; and (2) a detailed $^{187}Os/^{188}Os$ profile for contemporaneous Jurassic seawater allowing insight into the contributions of the various global inputs into the oceans at this time and therefore providing information regarding ocean connectivity during the Early Jurassic.

Currently, the timing of development of oceanic seaways during Pangaean separation is poorly constrained, with estimates that include both the Hettangian and Sinemurian. The Hispanic Corridor, an initially epicontinental, but later fully oceanic seaway, connected the western Tethyan and eastern Pacific oceans along the Central Atlantic rift zone (Smith and Tipper, 1986; Smith et al., 1990; Riccardi, 1991; Hallam and Wignall, 1997; Aberhan, 2001). Formed through separation of the Pangaean supercontinent, this proto-Atlantic seaway resulted from one of the most significant palaeogeographic reorganisations in Earth's history (Smith et al., 1990). Initially developing over rifting continental crust (Smith et al., 1994), this marine corridor signified the tectonic transition from rifting to drifting, prior to the formation of the Atlantic Ocean (Smith et al., 1990). In addition to the profound impact on ocean circulation and equatorial distribution of marine organisms at this time, the marine corridor acted as a filter during its early stages, preferentially allowing passage of on-shore benthic species, whilst acting as an effective barrier for off-shore species (eg. Hallam and Wignall, 1997; Smith et al., 1994; Aberhan, 2001). However, with no direct sedimentological or geophysical evidence, determining the timing for the establishment of the corridor using biogeography has been the subject of continuous debate. As such, the timing of seaway formation is currently imprecise and suggested to have occurred within the Early Jurassic (eg. Damborenea, 2000; Aberhan, 2001).

The $^{187}Os/^{188}Os$ values from the Sinemurian–Pliensbachian GSSP, Robin Hood's Bay, UK, provide evidence for significant low-temperature hydrothermal activity that may have been associated with the formation of the Hispanic Corridor during the breakup of Pangaea. Combined with biogeography and faunal exchange patterns, the Os data herein suggests that connectivity between the Eastern Pacific and Tethyan oceans initiated during the latest Sinemurian. Thus, this study better constrains the timing of establishment of the Hispanic Corridor, previously limited to poorly defined biogeography.

2. Geology of the Sinemurian–Pliensbachian boundary GSSP

Our study focuses on the marine sediments at the Sinemurian–Pliensbachian Global Boundary Stratotype Section and Point (GSSP) at Wine Haven, ~3 km S–SE of Robin Hood's Bay, Yorkshire, UK (Grid ref. NZ9762 0230 eg., Hesselbo et al., 2000; Meister et al., 2006; Fig. 1). This Lower Jurassic boundary occurs in the Pyritous Shales of the Redcar Mudstone Formation within the Lias Group (Powell, 1984). It has been the subject of scientific interest for many years, with the earliest reference to the site being by Young and Bird (1822). Exposure at Robin Hood's Bay is optimal, with lower beds exposed by a series of wave-cut platforms. The succession here is also known for its well-preserved ammonite assemblages (eg. Tate and Blake, 1876; Dommergues and Meister, 1992). Using ~~From~~ the biostratigraphy, the base of the Pliensbachian Stage can be unambiguously located at the bottom of the *taylori* Subzone of the *Uptonia j~~.~~amesoni* Zone, marked by the first occurrence of species of the genus *Apoderoceras* (Dean et al., 1961; Hesselbo et al., 2000; Gradstein et al., 2004; Meister et al., 2006).

Formatted: Font: Italic

Formatted: Font: Italic

Formatted: Font: Italic

The age for the base of the Pliensbachian has been defined by the Geological Time Scale (GTS) 2004 as 189.6 ± 1.5 Ma (Gradstein et al., 2004), derived from cycle-scaled linear Sr trends and ammonite occurrences (as noted above; also includes the lowest occurrence of *Bifericeras donovani*; Gradstein et al., 2004). Herein, this age for the Sinemurian–Pliensbachian boundary is used. The

Sinemurian–Pliensbachian boundary is placed very close to the base of Bed 73 (bed classification from Hesselbo and Jenkyns, 1995), ~6 cm above the midline of nodules forming the upper margin of Bed 72 in the Wine Haven section (Hesselbo et al., 2000).

An epicontinental sea, positioned to the west of the deep Tethyan basin (Dera et al., 2009) covered most of Northern Europe, including Britain, during the Mesozoic (Sellwood and Jenkyns, 1975; Fig. 1). Lithological evidence for sea level rise, combined with sedimentological evidence (Smith et al., 1994), indicates that the epicontinental sea during this time was not landlocked but free to circulate with the Tethyan ocean. The open ocean Os isotope composition across the boundary interval should therefore be echoed in the sampled sediments. Analysis of hydrogenous Re and Os from these samples instils certainty that the calculated initial Os isotope composition ($^{187}Os/^{188}Os_{(i)}$) reflects that of contemporaneous seawater (Cohen et al., 1999).

Over a ~10 m interval, the lithology of the Wine Haven succession gradually progresses from pale siliceous and clay-rich mudrocks with intermittent coarser sand beds in the Upper Sinemurian (Aplanatum Subzone), to finer and much darker shales with less clay ~1.5 m above the boundary in the Lower Pliensbachian (~~*Taylori*~~*taylori* Subzone; Meister et al., 2006; Hesselbo and Jenkyns, 1995, 1998; this study). These facies changes indicate an overall relative increase in sea level of at least regional, but possibly global extent (Sellwood, 1972; Hallam, 1981; Hesselbo and Jenkyns 1995, 1998; Hesselbo et al., 2000; Meister et al., 2006).

Formatted: Font: Italic

Nodular beds of concretionary siderite (~10 cm in thickness) of both laterally continuous (Beds 70 and 72) and semi-continuous extent (Bed 74 and within Bed 71) are present throughout the Wine Haven section (Sellwood, 1972; Meister et al., 2006; this study). The origin of these nodules is uncertain, although they are suggested to represent non- or slow depositional phases based on their unique association with fauna found in life-position (Sellwood, 1972).

Sedimentation rate across the Sinemurian–Pliensbachian boundary has been approximated here by taking ~64 Ma as the duration for the Jurassic period (Gradstein et al., 2004) and using mean thicknesses of ammonite zonal subdivisions estimated by Hallam and Sellwood (1976). This provides

a combined thickness for the Sinemurian and Pliensbachian of ~278 m, ~23 % of the total for the Jurassic. By disregarding the uncertain effects of compaction (Hallam and Sellwood, 1976), a steady sedimentation rate during this interval has been calculated at ~1.9 cm/Ka, in turn suggesting that the interval sampled by this study (~6 m) spans ~320 Ka.

Although the $^{87}Sr/^{86}Sr$ profile (Hesselbo et al., 2000) shows a systematic decrease up-section (~0.707487 to 0.707395 over a 10 m interval), a lack of any abrupt changes in the $^{87}Sr/^{86}Sr$ ratio indicates that sedimentation was continuous (Jones et al., 1994; Hesselbo et al., 2000; Meister et al., 2006). At the boundary level, a drop in $^{87}Sr/^{86}Sr$ value from ~0.707433 to 0.707418 (Hesselbo et al., 2000) could allow the possibility of minor slowing or hiatus in sediment deposition (Hesselbo et al., 2000; Meister et al., 2006). However, replicate analyses of belemnites from 1–4 cm above the boundary give an average $^{87}Sr/^{86}Sr$ value of 0.707422 ± 0.000012, well within uncertainty of the ratio recorded for the boundary (0.707425 ± 0.000004) (Hesselbo et al., 2000), suggesting a slowing rather than break in deposition (Hesselbo et al., 2000; Meister et al., 2006). Further evidence for continuous deposition is supported by a lack of lithological unconformities (Meister et al., 2006; this study).

3. Analytical methodology

3.1 Sampling

A set of 32 samples (SP7-09 to SP39-09) were collected from the Pyritous Shales Member of the Redcar Mudstone Formation, along a 6 m vertical section bracketing the Sinemurian–Pliensbachian boundary (sample SP22-09) at Robin Hood's Bay (Fig. 2). Sampling occurred at a consistent interval of ~20 cm for 3 m above and 3 m below the boundary from Beds 69–75 except within Bed 72, where a smaller sampling interval of ~15 cm was used (Fig. 2). Based on our approximation above for the duration of sedimentation across this section, sampling at ~20 cm intervals allowed us to capture an estimated resolution of ~11 Ka per sample.

In preparation for geochemical analyses, the samples were cut and polished to expose fresh surfaces, and were then powdered in a Zr disc.

3.2 Re-Os analysis

Rhenium and osmium analyses of Robin Hood's Bay whole-rock powders were conducted at the Japan Agency for Marine-Earth Science and Technology (JAMSTEC) as part of the JSPS Summer Fellowship Program 2010, following the CrO_3-H_2SO_4 procedure outlined by Selby and Creaser (2003). This digestion technique minimises removal of Re and Os from the nonhydrogenous (detrital) component of the sample, allowing analysis and evaluation of the hydrogenous fraction (Selby and Creaser, 2003). Sample powders of known quantities (500 mg for samples with >50 ppb Re or 1g for samples with <50 ppb Re) were digested with a measured amount of ^{185}Re and ^{190}Os spike solution, in 8 ml of CrO_3-H_2SO_4 solution in Carius tubes at 240 ^{o}C for 48 hrs. After cooling, Os was removed and purified from the solution by solvent extraction and micro-distillation.

Following Os removal, the remaining solution was prepared for anion exchange chromatography to purify the Re fraction. To reduce Cr^{6+} to Cr^{3+}, necessary to avoid complications during chromatography (Selby and Creaser, 2003), 1 ml of the remaining solution was removed and reduced drop by drop (due to the violent exothermic reaction) using 3 ml of ethanol (gradual addition of ethanol to the sample solution is advised to avoid loss of sample during the reduction reaction). Once reduced, the solution was evaporated to dryness on a hotplate at ~80^{o}C.

The dried Re fraction was taken up in a 10 ml 0.5 N HCl loading solution, before being purified by a two-stage HCl-HNO_3 anion chromatography procedure. The purified Re and Os was loaded onto Ni and Pt filaments, respectively and the Re and Os isotope ratios were measured using NTIMS (Creaser et al., 1991; Völkening et al., 1991) using Faraday collectors and the SEM, respectively. The initial Os isotope composition ($^{187}Os/^{188}Os_{(i)}$) was calculated using an independently assumed sample age of ~189.6 Ma (Gradstein et al., 2004) and $\lambda\ ^{187}Re = 1.666 \times 10^{-11}\ a^{-1}$ (Smoliar et al., 1996). During this study total procedural blanks were 14.1 ± 0.2 pg and 3.56 ± 0.52 pg (1σ S.D., n

= 2) for Re and Os, respectively, with an average $^{187}Os/^{188}Os$ value of 0.19 ± 0.005 (n = 2). Uncertainties presented in Table 1 include full error propagation of uncertainties in Re and Os mass spectrometer measurements, blank abundances and isotopic compositions, spike calibrations and reproducibility of standard Re and Os isotopic values.

4. Results

4.1 Re and Os abundance

The Re and Os abundances define a large range of values, from ~1.5–117 and ~0.12–1.9 ppb, respectively (Table 1). These values are much greater than those of average continental crust: 0.39 ppb (Re) and 0.05 ppb (Os) (Sun et al., 2003 and references therein). Both Re and Os abundances show an overall increase up-section that becomes more pronounced following the Sinemurian–Pliensbachian boundary.

4.2 Re-Os geochronology

In order to conduct Re-Os geochronology, the targeted samples should fulfil three criteria. Each sample must possess a similar initial Os isotope composition ($^{187}Os/^{188}Os_{(i)}$) together with variable $^{187}Re/^{188}Os$ ratios, and have experienced no disturbance to the isotope system since the time of formation (Cohen et al., 1999). The Robin Hood's Bay section shows no evidence of post-depositional disturbance, e.g., no veining is evident and the section is thermally immature. Similar Jurassic sections have been utilised for Re-Os geochronology (Cohen et al., 1999).

For the Robin Hood Bay section the $^{187}Re/^{188}Os$ and $^{187}Os/^{188}Os$ ratios vary from ~25–443 and ~0.3–1.6, respectively. Both $^{187}Re/^{188}Os$ and $^{187}Os/^{188}Os$ ratios decrease between 2.8 to 0.9 m below the Sinemurian–Pliensbachian boundary ($^{187}Re/^{188}Os$, ~195–20; $^{187}Os/^{188}Os$, ~1–0.3), before systematically increasing across the boundary into the lowermost Pliensbachian. Although all the $^{187}Re/^{188}Os$ and $^{187}Os/^{188}Os$ ratios positively correlated (R^2 = 0.95), the Re-Os data yield model 3 age

of 179 ± 16 Ma (2σ, n = 32, MSWD = 473; Fig. 4a). Although within uncertainty of the calculated age for the Sinemurian–Pliensbachian boundary (189.6 ± 1.5 Ma; Gradstein et al., 2004), the uncertainty is large (~9 %) and is accompanied by an extremely large MSWD, which indicates significant scatter of the data about the isochron that relates to more than analytical uncertainty. We suggest that this scatter relates to the sample set possessing variable initial $^{187}Os/^{188}Os$ values. The calculated initial $^{187}Os/^{188}Os$ ($^{187}Os/^{188}Os_{(i)}$ at 189.6 Ma; Gradstein et al., 2004) values for this Sinemurian–Pliensbachian section are variable, but consistently unradiogenic for all samples, ranging from ~0.20–0.48. Overall, with exceptions at 1.1 m below the boundary and at the boundary itself (sample SP22-09, $^{187}Os/^{188}Os_{(i)}$ = ~0.48 and SP17-09 = ~0.44, respectively; Fig. 3; 4b), the $^{187}Os/^{188}Os_{(i)}$ values become progressively less radiogenic up-section.

If we consider samples with similar $^{187}Os/^{188}Os_{(i)}$ values (~0.20–0.30) regression of the Re-Os data produces a model 3 age of 183.4 ± 3.3 Ma (2σ, n = 17, MSWD = 20; Fig. 4c). This age is outside of uncertainty of that given by Gradstein et al. (2004). Regression of Re-Os data for the top four stratigraphic organic-rich samples in the section (SP34-09, SP35-09, SP36-09 and SP37-09) provides a model 1 age of 194 ± 4.8 Ma (2σ, n = 4, MSWD = 0.04; Fig. 4d). These samples are ideally suited to Re-Os geochronology because they possess extremely similar initial $^{187}Os/^{188}Os$ compositions (~0.20–0.22) and variable $^{187}Re/^{188}Os$ ratios (~268–443). As such, the model age is within uncertainty of that given by Gradstein et al. (2004). Although the Robin Hood bay section is not ideally suited for Re-Os geochronology, the positive correlation of $^{187}Re/^{188}Os$ with $^{187}Os/^{188}Os$ that yields dates that are in agreement with the Geological Time Scale 2004 (Gradstein et al., 2004), suggests that the Re-Os systematics have not been disturbed and that calculated initial $^{187}Os/^{188}Os$ values can be used to discuss Early Jurassic ocean chemistry.

5. Discussion

The Jurassic was a dynamic period that hosted major geological events of Earth's history; notably the full-scale tectonic plate reorganisation associated with the break-up of Pangaea. Ocean chemistry was therefore subject to fluctuations as the balance of inputs changed, and as such the seawater Os isotope composition was highly variable. In order to look critically at the data herein and to determine the potential source of the Os isotope signal observed across the Sinemurian–Pliensbachian boundary, there needs to be an understanding of the background seawater Os isotope composition at this time. However, at present no studies conclusively document background seawater Os for the Early Jurassic. The first estimation of stable, steady-state $^{187}Os/^{188}Os$ values for the Sinemurian is proposed to be ~ 0.47 (Kuroda et al., 2010). The sampled section (Triassic–Jurassic chert succession from Kurusu, Japan; Kuroda et al., 2010) was positioned to the east of the separating supercontinent, in an intra-ocean setting. The recorded Os isotope composition would therefore not have been directly affected by nearby continental flux, and would have been a good representation of open ocean chemistry at this time. For this investigation, we will assume that this value represents the best estimation of background seawater Os isotope composition at the Sinemurian–Pliensbachian transition.

5.1 Origin of the Sinemurian–Pliensbachian seawater Os isotope composition

The Os data from Robin Hoods Bay show that the calculated seawater initial $^{187}Os/^{188}Os$ value becomes progressively more unradiogenic from the latest Sinemurian into the Pliensbachian. Although there is some fluctuation, this trend to unradiogenic values can be broadly separated into three groups, with average $^{187}Os/^{188}Os_{(i)}$ values of ~0.38, 0.28 and 0.21 (Fig. 3). These results indicate that there was a marked and progressive increase of unradiogenic Os input into the global ocean during the transition from the Sinemurian to the Pliensbachian.

A peak towards a relatively radiogenic $^{187}Os/^{188}Os$ value of 0.48 is coincident with the boundary. This is also matched by an increase in the $^{187}Re/^{188}Os$ ratio (from ~31 to 100) and a

decrease in ^{192}Os (from ~208 to 102 ppb). Assuming a background seawater Os isotope composition of ~0.47 (Kuroda et al., 2010), this peak may reflect a period of hiatus in the input of unradiogenic Os to the oceans.

There are three major inputs of Os that directly control the seawater $^{187}Os/^{188}Os$ value: (1) radiogenic input from weathering of continental crust; (2) unradiogenic contribution from meteorites; (3) an unradiogenic signal from igneous and hydrothermal activity (eg. Peucker-Ehrenbrink and Ravizza, 2000).

5.1.1 Why is the signal not induced by continental weathering?

The gradual trend towards unradiogenic Os isotope values observed in this study indicates that continental weathering is unlikely to be the cause of the Os isotopic signal shown over Sinemurian–Pliensbachian boundary. Belemnite oxygen stable isotope data displays a marked increase of ~1 ‰ over 10 m across the boundary (Hesselbo et al., 2000; Fig. 3). This 1 ‰ change is equivalent to a substantial temperature decrease of ~5^{o}C (Hesselbo et al., 2000; Meister et al., 2006). Such considerable lowering of temperature, coupled with evidence for low mean land relief and absence of ice sheets during the Early Jurassic (Golonka et al., 1994), would favour reduced rates of regional and global continental weathering.

The Os isotope signal resulting from continental weathering is also significantly more radiogenic ($^{187}Os/^{188}Os$ = ~1.4; Peucker-Ehrenbrink and Jahn, 2001) than that observed in this study. This indicates that the seawater Os isotope composition was dominated by an unradiogenic source that outweighed the input of radiogenic Os from continental weathering. It is extremely difficult to constrain the exact continental $^{187}Os/^{188}Os$ input to the oceans during the Early Jurassic. However, following Cohen et al. (1999), we can attempt to quantify the approximate contribution of crustal Os into the ocean. Assuming an average $^{187}Os/^{188}Os$ value of ~1.4 for weathering of ancient continental crust (Peucker-Ehrenbrink and Jahn, 2001), and a $^{187}Os/^{188}Os$ value of ~0.13 for an unradiogenic mantle-derived source (Allègre and Luck, 1980; Esser and Turekian, 1993; Sharma et al., 1997;

292 Levasseur et al., 1998), an input of crustal-sourced Os of 5–22 % is required to obtain seawater
293 $^{187}Os/^{188}Os$ ratios of ~0.44–0.20, respectively. This is small in contrast to the present-day radiogenic
294 contribution to the oceans from the continental crust, of between ~ 70 and 80 % (Peucker-
295 Ehrenbrink, 1996; Sharma et al. 1997), respectively. Given the geographical location of Robin Hood's
296 Bay in close-proximity to continental landmasses (Fig. 5), and the absence of ice sheets, there would
297 almost certainly be radiogenic continental input regardless of land-relief and climate. Further,
298 although challenging to quantify, the epicontinental setting would mean increased sensitivity to
299 continental input. There is no evidence for the weathering of unradiogenic lithologies, e.g., mafic
300 and ultramafic units, thus the decrease in seawater $^{187}Os/^{188}Os$ composition during the earliest
301 Pliensbachian therefore indicates that input of Os into the ocean at this time was dominated by an
302 unradiogenic source, not accounted for by the continental weathering flux.
303
304 *5.1.2 Why is the unradiogenic Os not from an extraterrestrial source?*
305 Extraterrestrial and mantle-derived influxes are the dominant unradiogenic sources of Os to
306 the global oceans. The calculated $^{187}Os/^{188}Os$ values of these sources (~0.13) are indistinguishable
307 (Allègre and Luck, 1980; Esser and Turekian, 1993; Sharma et al., 1997; Levasseur et al., 1998). It is
308 therefore necessary to examine the structure of the Os isotope profiles from each source to
309 determine which was responsible for the declining unradiogenic Os signal into the Pliensbachian.
310 Fluctuations in the seawater Os isotope record during the Cenozoic were not induced by
311 extraterrestrial Os influx to the oceans, as the cosmic Os flux was continuous relative to the variable
312 ocean Os record (with the exception of the K–T boundary; Peucker-Ehrenbrink and Ravizza, 2000).
313 Although the extraterrestrial flux to Earth during the Jurassic is poorly constrained, the possibility of
314 meteorite impact at the Sinemurian–Pliensbachian boundary does not reconcile the gradual decline
315 in $^{187}Os/^{188}Os$ ratios. Following an impact, the Os isotope system should recover quickly due to the
316 relatively short seawater residence time of Os (Peucker-Ehrenbrink and Ravizza, 2000). Therefore,
317 although impacts have been documented ~5–20 Ma prior to the Triassic – Jurassic boundary (Hallam

and Wignall, 1997), it would be unlikely to find evidence of meteoritic unradiogenic Os during the Pliensbachian. This is further supported by a study of the Os isotope excursion due to meteorite impact across the K–T boundary (Ravizza and Peucker-Ehrenbrink, 2003), that shows relatively rapid recovery of the Os isotope system to a steady state following impact ($^{187}Os/^{188}Os$ value increases from ~0.16 to 0.40 in a maximum of ~200 Ka).

5.1.3 Unradiogenic Os from a mantle-derived source

The unradiogenic $^{187}Os/^{188}Os$ values are therefore most likely to be mantle-derived. Unlike the other potential sources of oceanic Os discussed above, increased input from a mantle source at the time of the Sinemurian–Pliensbachian boundary can explain the observed isotope profiles.

Rifting of the Pangaean Supercontinent began during the latest Triassic (Marzoli et al., 1999; Hames et al., 2000). The initial stages of continental break-up were focused along the 6000 km lineament that would eventually form the continental margins of the Central North Atlantic Ocean (Hames et al., 2000). Consequently, there is evidence for substantial magmatism during the Late Triassic–Early Jurassic (Marzoli et al., 1999; Hames et al., 2000), defined by extensive continental basalts in North America, Europe, Africa and South America (Wilson, 1997; Marzoli et al., 1999). This formed what is termed as the Central Atlantic Magmatic Province (CAMP). The scale of the CAMP has been postulated to exceed that of the Karoo-Ferrar, the Deccan Traps and the Siberian continental flood basalt provinces (Hames et al., 2000), with a total areal extent and volume of at least 7×10^6 Km^2 and 2×10^6 km^3, respectively (Marzoli et al., 1999; Hames et al., 2000).

High-precision $^{40}Ar/^{39}Ar$ geochronology of the oldest CAMP volcanic rocks, indicate that emplacement occurred during the transition from Late Triassic to Early Jurassic (ca. 200 Ma) with a brief duration of ~ < 2 Ma (Marzoli et al., 1999; Hames et al., 2000). A volcanic event of this magnitude, considering both its sizeable magmatic and hydrothermal outputs, would have had a considerable impact on ocean chemistry, regardless of its exceptionally brief duration (Ravizza and Peucker-Ehrenbrink, 2003). This has been documented by several Os isotope studies of seawater at

the Triassic–Jurassic boundary and during the Hettangian (Cohen et al., 1999; Cohen and Coe, 2002; Cohen, 2004). Prior to and immediately following the Triassic–Jurassic boundary, there was a significant unradiogenic contribution of Os to the oceans that persisted into the Hettangian (Cohen et al., 1999; Cohen and Coe, 2002; Cohen, 2004). This has been attributed to seawater interaction and alteration of recently emplaced CAMP lavas, together with enhanced hydrothermal activity (Cohen et al., 1999; Cohen and Coe, 2002; Cohen, 2004). High chemical weathering rates of juvenile basalts (Louvat and Allègre, 1997) characteristically promote relatively rapid release of unradiogenic Os, which can be seen in the Triassic–Jurassic and Hettangian sample suites (Cohen et al., 1999; Cohen and Coe, 2002; Cohen, 2004). The seawater Os isotopic composition then becomes increasingly unradiogenic across the Sinemurian–Pliensbachian boundary, to $^{187}Os/^{188}Os$ ratios of ~0.20. Using estimates for Early Jurassic stage durations from Gradstein et al. (2004), this boundary occurred ~ 10 Ma after the Triassic–Jurassic boundary and at least ~8 Ma after emplacement of CAMP. Further, the total duration of weathering of CAMP basalts is estimated at ~3.5 Ma (Cohen and Coe, 2007), producing a seawater $^{187}Os/^{188}Os$ value of ~0.30. It is therefore difficult to reconcile the observed Sinemurian–Pliensbachian seawater Os isotope composition with the CAMP emplacement event (ca. 200 Ma) or weathering of the continental flood basalts, given a date for the Sinemurian–Pliensbachian stage boundary of 189.6 ± 1.5 Ma (Gradstein et al., 2004).

However, when considering palaeogeographic and biogeographic evidence, it is possible to determine a mantle-derived origin for the unradiogenic seawater Os isotope composition that does not rely on emplacement of CAMP lavas. Hydrothermal activity would have been prevalent in this tectonic setting, and low temperature hydrothermal fluids have a characteristically unradiogenic Os isotope composition of ~0.12 (Cohen et al., 1999; Sharma et al., 2000).

5.2 Os isotope evidence for oceanic connectivity via the 'Hispanic Corridor' during the Early Pliensbachian

The separation of Pangaea and onset of a global sea level rise established a number of epeiric seaways, including the Hispanic Corridor (Aberhan, 2001). This initially epicontinental, but later fully oceanic seaway was established along the Central Atlantic rift zone, between the areas of North America, South America and Africa (Smith and Tipper, 1986), eventually connecting the western Tethyan and eastern Pacific oceans (eg. Smith and Tipper, 1986; Smith et al., 1990; Riccardi, 1991; Aberhan, 2001; Fig. 5).

No connectivity existed between these oceans during the Hettangian or Sinemurian, providing an effective barrier to oceanic circulation and thus to faunal exchange (eg. Smith and Tipper, 1986; Riccardi, 1991; Aberhan, 2001). In addition, biogeographic and sedimentological evidence indicates that an oceanic corridor did not develop before the Middle Jurassic (Aberhan, 2001). Whilst some studies, based on benthic faunas, postulate an opening time for the corridor of Late Triassic (Sandy and Stanley, 1993) and early Hettangian (Sha, 2002), substantial evidence for sudden low levels of faunal exchange between the eastern Pacific and western Tethyan oceans exists in the earliest Pliensbachian (Damborenea and Manceñido, 1979; Smith and Tipper, 1986; Smith et al., 1990). This suggests establishment of the Hispanic Corridor as a shallow but continuous seaway by the start of the Pliensbachian. Schootbrugge et al. (2005) also suggest that short bursts in the diversification of dinoflagellates during the latest Sinemurian are consistent with the opening of this seaway.

The decline of seawater $^{187}Os/^{188}Os$ ratios and the rise in sea level evident across the Sinemurian–Pliensbachian boundary section at Wine Haven, are therefore coincident with the onset of flooding of the Hispanic Corridor. Furthermore, this study suggests that the isotopic signals observed at the boundary reflect increasing hydrothermal activity associated with the opening of the Hispanic Corridor.

394 The Hispanic Corridor developed across rifting continental crust (Smith et al., 1994), with
395 significant crustal stretching and attenuation occurring before creation of the oceanic strait (Hallam
396 and Wignall, 1997). Growing evidence also indicates that substantial off-axis hydrothermal venting
397 may occur in cooler crustal regions away from the immediate rift zone, driven by exothermic
398 reactions between seawater and mantle-derived rocks (Kelley et al., 2001). This is evident at the
399 Mid-Atlantic and Juan de Fuca ridges, respectively (Kelley et al., 2001; Sharma et al., 2000),. Off-axis
400 fluids are typically cool (~40–75°C) with high Os concentrations (~500 femtomol/kg) and
401 unradiogenic $^{187}Os/^{188}Os$ ratios of ~0.12 (Sharma et al., 2000). Mantle-derived material (basalt) was
402 prevalent in this Central Atlantic region (eg. Wilson, 1997; Marzoli et al., 1999), allowing seawater-
403 rock interaction to ensue following the initial flooding event. This would have driven extensive low-
404 temperature hydrothermal fluid circulation, promoting an increase in the release of unradiogenic Os
405 into the seawater (Sharma et al., 2000).
406
407
408 **6. Conclusions**

409 The Sinemurian–Pliensbachian boundary GSSP at Robin Hood's Bay, UK, has the potential to
410 provide a significantly increased understanding of seawater chemistry during the Early Jurassic.
411 Further, understanding changes in ocean chemistry during this time has the potential to yield
412 valuable insight into ocean connectivity during Pangaean separation.
413 Seawater during the Sinemurian–Pliensbachian transition became dominated by an
414 unradiogenic $^{187}Os/^{188}Os$ signal that is not resolvable by influxes from continental weathering or
415 meteorite impact. The break-up of Pangaea was of fundamental importance to this observed
416 isotopic trend, and a mantle-derived source favours the constructed Os isotope profile.
417 The Triassic–Jurassic boundary marks the onset of volcanism in the Central Atlantic
418 Magmatic Province, directly associated with Pangaean fragmentation. Following this there is strong
419 taxonomic evidence for sudden, albeit restricted levels, of faunal exchange between the western

Tethyan and eastern Pacific oceans in the latest Sinemurian and the start of the Pliensbachian, via the Hispanic Corridor (defining the rift zone between North America, South America and Africa). This stage boundary therefore marks the initial flooding event of the Hispanic Corridor that also corresponds to an on-going global sea level rise. Seawater inundation would have initiated seawater interaction with, and circulation into, deep crustal fissures associated with rifting in this region, thus driving extensive low-temperature hydrothermal activity. Such low-temperature hydrothermal fluids are characterised by unradiogenic $^{187}Os/^{188}Os$ ratios of ~0.12 (Sharma et al., 2000; Kelley et al., 2001). It is therefore possible that the unradiogenic $^{187}Os/^{188}Os$ signal observed across the Sinemurian–Pliensbachian boundary marks the onset of hydrothermal activity associated with formation of the Hispanic Corridor.

Acknowledgments

This research was supported through the JSPS Summer Fellowship Program, hosted by the Japan Agency for Marine-Earth Science and Technology (JAMSTEC) and a NERC PhD studentship to SJP. Thanks to Katz Suzuki, Ryoko Senda and Akira Ishikawa for their assistance in the laboratory.

Figure captions

Fig. 1. Map showing the European epicontinental sea and the geographical relationship between the Hispanic Corridor, Tethyan Ocean and Robin Hood's Bay. Modified after Dera et al. (2009). A location map of the Wine Haven section is also provided.

Fig. 2. Graphic log showing the Sinemurian–Pliensbachian boundary GSSP and the relative locations of the samples analysed in this study. Bed number classification taken from Hesselbo and Jenkyns (1995).

Fig. 3. Re-Os isotope stratigraphy across the Sinemurian–Pliensbachian boundary GSSP, UK. Strontium isotope ($^{87}Sr/^{86}Sr$) from Jones et al. (1994) and Hesselbo et al. (2000), and $\delta^{18}O$ data from Hesselbo et al. (2000). Grey dashed line, A, reflects the three groups of $^{187}Os/^{188}Os_{(i)}$ values for seawater across the Sinemurian–Pliensbachian boundary (~0.38, 0.28 and 0.21). Black dashed line, B[1], represents the first estimation of stable steady-state $^{187}Os/^{188}Os$ values for Early Jurassic seawater (~0.47; Kuroda et al., 2010). Bed number classification taken from Hesselbo and Jenkyns (1995).

Fig. 4. a) Rhenium-osmium isochron for all Robin Hood's Bay samples (n = 32); **b)** Histogram showing the variability of the initial $^{187}Os/^{188}Os$ ratio in the Robin Hood's Bay sediments, calculated at 189.6 Ma; **c)** All Robin Hood's Bay samples with initial $^{187}Os/^{188}Os$ ratios between ~0.20 – 0.30 (n = 17); **d)** The four samples at the top of the studied Robin Hood's Bay section, with variable $^{187}Re/^{188}Os$ ratios (~268 – 443) and similar initial $^{187}Os/^{188}Os$ ratios (~0.20 – 0.22).

Fig. 5. Global reconstruction of Pangaea in the Early Jurassic. Map shows the relative locations of the Central Atlantic Magmatic Province (CAMP), the Hispanic Corridor, the Tethyan and Pacific oceans and Robin Hood's Bay. Modified after www.scotese.com.

Table 1. Re and Os isotope data for the Sinemurian–Pliensbachian boundary GSSP, UK.

References

Aberhan, M., 2001. Bivalve palaeobiogeography and the Hispanic Corridor: time of opening and effectiveness of a proto-Atlantic seaway. Palaeogeography, Palaeoclimatology, Palaeoecology 165, 375-394.

Allègre, C.J., Luck, J.-M., 1980. Osmium isotopes as petrogenetic and geological tracers. Earth and Planetary Science Letters 48, 148-154.

Cohen, A.S., 2004. The rhenium-osmium isotope system: applications to geochronological and palaeoenvironmental problems. Journal of the Geological Society of London 161, 729-734.

Cohen, A.S., Coe, A.L., 2002. New geochemical evidence for the onset of volcanism in the central Atlantic magmatic province and environmental change at the Triassic–Jurassic boundary. Geology 30, 267-270.

Cohen, A.S., Coe, A.L., 2007. The impact of the Central Atlantic Magmatic Province on climate and on the Sr- and Os-isotope evolution of seawater. Palaeogeography, Palaeoclimatology, Palaeoecology 244, 374-390.

Cohen, A.S., Coe, A.L., Bartlett, J.M., Hawkesworth, C.J., 1999. Precise Re-Os ages of organic-rich mudrocks and the Os isotope composition of Jurassic seawater. Earth and Planetary Science Letters 167, 159-173.

Creaser, R.A., Papanastassiou, D.A., Wasserburg, G.J., 1991. Negative thermal ion mass spectrometry of osmium, rhenium and iridium. Geochimica et Cosmochimica Acta 55, 397-401.

Damborenea, S.E., 2000. Hispanic Corridor: Its evolution and biogeography of bivalve molluscs. In: Hall, R., Smith, P.L. (Eds.), Advances in Jurassic Research 2000. Proceedings of the Fifth International Symposium on the Jurassic System, Trans Tech, Switzerland. GeoResearch Forum, pp. 369-380.

Damborenea, S.E., Manceñido, M.O., 1979. On the palaeogeographical distribution of the pectinid genus Weyla (Bivalvia, lower Jurassic). Palaeogeography, Palaeoclimatology, Palaeoecology 27, 85-102.

Dean, W.T., Donovan, D.T., Howarth, M.K., 1961. The Liassic ammonite Zones and Subzones of the North West European Province. Bulletin of the Natural History Museum 4, 435-505.

Dera, G., Pucéat, E., Pellenard, P., Neige, P., Delsate, D., Joachimski, M.M., Reisberg, L., Martinez, M., 2009. Water mass exchange and variations in seawater temperature in the NW Tethys during the Early Jurassic: Evidence from neodymium and oxygen isotopes of fish teeth and belemnites. Earth and Planetary Science Letters 286, 198-207.

Dommergues, J.-L., Meister, C., 1992. Late Sinemurian and Early Carixian ammonites in Europe with cladistic analysis of sutural characteristics. Neues Jahrbuch fur Geologie and Palaontologie Abhandlungen 185, 211-237.

Esser, B.K., Turekian, K.K., 1993. The osmium isotopic composition of the continental crust. Geochimica et Cosmochimica Acta 57, 3093-3104.

Golonka, J., Ross, M.I., Scotese, C.R., 1994. Phanerozoic paleogeographic and paleoclimatic modeling maps. In: Embry, A.F., Beauchamp, B., Glass, D.J. (Eds.), Pangaea: Global environments and resources. Canadian Society of Petroleum Geologists Memoir 17, 1-47.

Gradstein, F.M., Ogg, J.G., Smith, A.G., Bleeker, W., Lourens, L.J., 2004. A new Geologic Time Scale, with special reference to Precambrian and Neogene. Episodes 27, 83-100.

Hallam, A., 1981. A revised sea-level cruve for the early Jurassic. Journal of the Geological Society of London 138, 735-743.

Hallam, A., Sellwood, B.W., 1976. Middle Mesozoic Sedimentation in Relation to Tectonics in the British Area. Journal of Geology 84, 301-321.

Hallam, A., Wignall, P.B., 1997. Mass Extinctions and Their Aftermath. Oxford University Press, Oxford.

Hames, W.E., Renne, P.R., Ruppel, C., 2000. New evidence for geologically instantaneous emplacement of earliest Jurassic Central Atlantic Magmatic Province basalts on the North American margin. Geology 28.

Hesselbo, S.P., Jenkyns, H.C., 1995. A comparison of the Hettangian to Bajocian successions of Dorset and Yorkshire. In: Taylor, P.D. (Ed.), Field Geology of the British Jurassic. Geological Society of London, pp. 105-150.

Hesselbo, S.P., Jenkyns, H.C., 1998. British Lower Jurassic Sequence Stratigraphy. In: De Graciansky, P.C., Hardenbol, J., Jacquin, T., Vail, P.R. (Eds.), Mesozoic and Cenozoic Sequence Stratigraphy of European Basins. Special Publication of the Society for Sedimentary Geology (SEPM) 60, pp. 561-581.

Hesselbo, S.P., Meister, C., Gröcke, D.R., 2000. A potential global stratotype for the Sinemurian–Pliensbachian boundary (Lower Jurassic), Robin Hood's Bay, UK: ammonite faunas and isotope stratigraphy. Geological Magazine 137, 601-607.

Jones, C.E., Jenkyns, H.C., 2001. Seawater strontium isotopes, oceanic anoxic events, and seafloor hydrothermal activity in the Jurassic and Cretaceous. American Journal of Science 301, 112-149.

Jones, C.E., Jenkyns, H.C., Hesselbo, S.P., 1994. Strontium isotopes in Early Jurassic seawater. Geochimica et Cosmochimica Acta 58, 1285-1301.

Kelley, D.S., Karson, J.A., Blackman, D.K., Fruh-Green, G.L., Butterfield, D.A., Lilley, M.D., Olson, E.J., Schrenk, M.O., Roe, K.K., Lebon, G.T., Rivizzigno, P., Party, A.-S., 2001. An off-axis hydrothermal vent field near the Mid-Atlantic Ridge at 30°N. Nature 412, 145-149.

Kuroda, J., Hori, R.S., Suzuki, K., Gröcke, D.R., Ohkouchi, N., 2010. Marine osmium isotope record across the Triassic–Jurassic boundary from a Pacific pelagic site. Geology 38, 1095-1098.

Levasseur, S., Birck, J.-L., Allègre, C.J., 1998. Direct Measurement of Femtomoles of Osmium and the $^{187}Os/^{186}Os$ Ratio in Seawater. Science 282, 272-274.

Levasseur, S., Birck, J.L., Allègre, C.J., 1999. The osmium riverine flux and the oceanic mass balance of osmium. Earth and Planetary Science Letters 174, 7-23.

Louvat, P., Allègre, C.J., 1997. Present denudation rates on the island of Réunion determined by river geochemistry: Basalt weathering and mass budget between chemical and mechanical erosions. Geochimica et Cosmochimica Acta 61, 3645-3669.

Marzoli, A., Renne, P.R., Piccirillo, E.M., Ernesto, M., Bellieni, G., De Min, A., 1999. Extensive 200-Million-Year-Old Continental Flood Basalts of the Central Atlantic Magmatic Province. Science 284, 616-618

Meister, C., Aberhan, M., Blau, J., Dommergues, J.-L., Feist-Burkhardt, S., Hailwood, E.A., Hart, M., Hesselbo, S.P., Hounslow, M.W., Hylton, M., Morton, N., Page, K., Price, G.D., 2006. The Global Boundary Stratotype Section and Point (GSSP) for the base of the Pliensbachian Stage (Lower Jurassic), Wine Haven, Yorkshire, UK. Episodes 29, 93-114.

Oxburgh, R., 1998. Variations in the osmium isotope composition of sea water over the past 200,000 years. Earth and Planetary Science Letters 159, 183-191.

Palmer, M.R., Falkner, K.K., Turekian, K.K., Calvert, S.E., 1988. Sources of osmium isotopes in manganese nodules. Geochimica et Cosmochimica Acta 52, 1197-1202.

Peucker-Ehrenbrink, B., 1996. Accretion of extraterrestrial matter during the last 80 million years and its effect on the marine osmium isotope record. Geochimica et Cosmochimica Acta 60, 3187-3196.

Peucker-Ehrenbrink, B., Jahn, B., 2001. Rhenium-osmium isotope systematics and platinum group element concentrations: Loess and the upper continental crust. Geochemistry, Geophysics, Geosystems 2, 1061-1083.

Peucker-Ehrenbrink, B., Ravizza, G., 2000. The marine osmium isotope record. Terra Nova 12, 205-219.

Powell, J.H., 1984. Lithostratigraphical nomenclature of the Lias Group in the Yorkshire Basin. Proceedings of the Yorkshire Geological Society 45, 51-57.

568 Ravizza, G., Martin, C.E., German, C.R., Thompson, G., 1996. Os isotopes as tracers in seafloor
569 hydrothermal systems: metalliferous deposits from the TAG hydrothermal area, 26°N Mid-
570 Atlantic Ridge. Earth and Planetary Science Letters 138, 105-119.
571 Ravizza, G., Peucker-Ehrenbrink, B., 2003. Chemostratigraphic Evidence of Deccan Volcanism from
572 the Marine Osmium Isotope Record. Science 302, 1392-1395.
573 Riccardi, A.C., 1991. Jurassic and Cretaceous marine connections between the Southeast Pacific and
574 Tethys. Palaeogeography, Palaeoclimatology, Palaeoecology 87, 155-189.
575 Sandy, M. R., Stanley, G.D., 1993. Late Triassic brachiopods from the Luning Formation, Nevada, and
576 their paleogeographical significance. Palaeontology 36, 439-480.
577 Schootbrugge, B., Bailey, T.R., Rosenthal, Y., Katz, M.E., Wright, J.D., Miller, K.G., Feist-Burkhardt, S.,
578 Falkowski, P.G., 2005. Early Jurassic climate change and the radiation of organic-walled
579 phytoplankton in the Tethys Ocean. Paleobiology 31, 73-97.
580 Selby, D., Creaser, R.A., 2003. Re-Os geochronology of organic rich sediments: an evaluation of
581 organic matter analysis methods. Chemical Geology 200, 225-240.
582 Sellwood, B.W., Jenkyns, H.C., 1975. Basins and swells and the evolution of an epeiric sea
583 (Pliensbachian-Bajocian of Great Britain). Journal of the Geological Society of London 131,
584 373-388.
585 Sellwood, W., 1972. Regional environmental changes across a Lower Jurassic stage-boundary in
586 Britain. Palaeontology 15, 125-157.
587 Sha, J., 2002. Hispanic Corridor formed as early as Hettangian: On the basis of bivalve fossils. Chinese
588 Science Bulletin 47, 414-417.
589 Sharma, M., Papanastassiou, D.A., Wasserburg, G.J., 1997. The concentration and isotopic
590 composition of osmium in the oceans. Geochimica et Cosmochimica Acta 61, 3287-3299.
591 Sharma, M., Wasserburg, G.J., Hofmann, A.W., Butterfield, D.A., 2000. Osmium isotopes in
592 hydrothermal fluids from the Juan de Fuca Ridge. Earth and Planetary Science Letters 179,
593 139-152.
594 Smith, A.G., Smith, D.G., Funnell, B.M., 1994. Atlas of Mesozoic and Cenozoic Coastlines. Cambridge
595 University Press.
596 Smith, P.L., Tipper, H.W., 1986. Plate Tectonics and Paleobiogeography: Early Jurassic (Pliensbachian)
597 Endemism and Diversity. Palaios 1, 399-412.
598 Smith, P.L., Westermann, G.E.G., Stanley, G.D., Jr., Yancey, T.E., Newton, C.R., 1990.
599 Paleobiogeography of the Ancient Pacific. Science 249, 680-683.
600 Smoliar, M.I., Walker, R.J., Morgan, J.W., 1996. Re-Os Ages of Group IIA, IIIA, IVA, and IVB Iron
601 Meteorites. Science 23, 1099-1102.

602 Sun, W., Bennett, V.C., Eggins, S.M., Kamenetsky, V.S., Arculus, R.J., 2003. Enhanced mantle-to-crust
603 rhenium transfer in undegassed arc magmas. Nature 422, 294-297.
604 Tate, R., Blake, J.F., 1876. The Yorkshire Lias. J. van Voorst, London.
605 Völkening, J., Walczyk, T., G. Heumann, K., 1991. Osmium isotope ratio determinations by negative
606 thermal ionization mass spectrometry. International Journal of Mass Spectrometry and Ion
607 Processes 105, 147-159.
608 Wilson, M., 1997. Thermal evolution of the Central Atlantic passive margins: continental break-up
609 above a Mesozoic super-plume. Journal of the Geological Society of London 154, 491-495.
610 Young, G.M., Bird, J., 1822. A geological survey of the Yorkshire Coast: describing the strata and
611 fossils occurring between the Humber and the Tees, from the German Ocean to the Plain of
612 York. Whitby. 366.
613
614 www.scotese.com (Figure 5: Pangaean reconstruction in the Early Jurassic)

Opening of a trans-Pangean marine corridor during the Early Jurassic: Insights from osmium isotopes across the Sinemurian-Pliensbachian GSSP, Robin Hood's Bay, UK.

Highlights

- New Re-Os isotope data across the Sinemurian-Pliensbachian boundary GSSP
- Os isotope composition of seawater becomes increasingly unradiogenic at this time
- Osmium isotopes indicate significant hydrothermal contribution to global seawater
- Osmium data indicates ocean connectivity via Hispanic Corridor in Latest Sinemurian

Opening of a trans-Pangaean marine corridor during the Early Jurassic: Insights from osmium isotopes across the Sinemurian–Pliensbachian GSSP, Robin Hood's Bay, UK.

Sarah J. Porter [a, *], David Selby [a], Katsuhiko Suzuki [b], Darren Gröcke [a]

[a] *Department of Earth Sciences, Durham University, Durham, DH1 3LE, UK.*
[b] *Japan-Agency for Marine-Earth Science and Technology, Yokosuka, 237-0061, Japan.*
[*] *Corresponding author (S. J. Porter). Tel.: +44 (0)191 334 2300; fax: +44 (0191) 334 2301; E-mail: sporter@eos.ubc.ca*

Keywords: Osmium isotopes, Hispanic Corridor, Sinemurian–Pliensbachian, organic-rich sediments, ocean connectivity

ABSTRACT

The Hispanic Corridor represents a significant phase of continental reorganisation of the Early Jurassic that eventually provided connectivity between the western Tethyan and eastern Pacific oceans along the Central Atlantic rift zone. Although the initiation of this marine corridor profoundly impacted oceanic circulation and marine faunal exchange patterns, the timing of its formation hitherto remains poorly constrained with estimates spanning both the Hettangian and Sinemurian. The Sinemurian–Pliensbachian Global Stratotype Section and Point (GSSP) at Robin Hood's Bay, UK, comprises a succession of well-exposed, immature organic-rich sediments, only previously characterised by strontium, oxygen and carbon isotope geochemistry. New Re and Os isotope profiling indicates substantial variation in seawater chemistry at this time. Initial osmium isotope data become increasing unradiogenic (0.40 to 0.20) across the boundary, providing evidence for a continual flux of unradiogenic Os into the oceans during the latest Sinemurian. The initial unradiogenic $^{187}Os/^{188}Os$ values indicate the occurrence of low-temperature hydrothermal activity associated with the formation of the Hispanic Corridor during the breakup of Pangaea. Therefore, combined with biogeography and faunal exchange patterns, the Os isotope data demonstrates that connectivity between the Eastern Pacific and Tethyan oceans initiated during the latest Sinemurian.

As a result this study better constrains the timing of establishment of the Hispanic Corridor, which was previously limited to poorly defined biogeography.

1. Introduction

Marine sedimentary rocks hold the key to understanding past chemical changes and fluxes in the oceans. Analysis of hydrogenous rhenium (Re) and osmium (Os) in organic-rich sediments allows detailed evaluation of seawater chemistry at the time of sediment deposition. The Os isotope system ($^{187}Os/^{188}Os$) is a particularly powerful tool for tracing temporal changes in the balance of global inputs to the oceans (Ravizza et al., 1996; Levasseur et al., 1999; Cohen et al., 1999; Peucker-Ehrenbrink and Ravizza, 2000), and as such it permits the evaluation of fluctuations in seawater chemistry throughout geological time. Specifically, significant input from meteorite impact, continental weathering and mantle-derived fluxes can be identified and distinguished.

The present-day seawater Os isotope composition may be relatively uniform ($^{187}Os/^{188}Os$ ratio of ~1.06; Levasseur et al., 1998; Peucker-Ehrenbrink and Ravizza, 2000), but it has varied significantly throughout geological time. The short seawater residence time of Os of ~10–40 Ka (Sharma et al., 1997; Oxburgh, 1998; Levasseur et al., 1998; Peucker-Ehrenbrink and Ravizza, 2000), longer than the mixing time of the oceans (~2–4 Ka; Palmer et al., 1988), allows the Os isotope composition to respond rapidly to any alterations in the composition and flux of these inputs (Oxburgh, 1998; Cohen et al., 1999). This has been successfully exploited by past studies, where Os has been used as a chemostratigraphic marker of significant volcanic events (eg., Cohen et al., 1999; Ravizza and Peucker-Ehrenbrink, 2003).

Until now, isotope stratigraphy of the Sinemurian–Pliensbachian GSSP at Robin Hood's Bay (Wine Haven, UK) has been limited to $^{87}Sr/^{86}Sr$ (Jones et al., 1994; Hesselbo et al., 2000), $\delta^{18}O$ and $\delta^{13}C$ data (Hesselbo et al., 2000) from belemnites. Herein we compile these datasets with Re-Os data, to provide new Os isotope characterisation of the Sinemurian–Pliensbachian GSSP. The longer

58 seawater residence time of Sr (~2.4 Ma; Jones and Jenkyns, 2001) relative to Os, slows the response
59 of Sr ratios to changes in the balances of inputs to the oceans (eg. Cohen and Coe, 2002). Therefore,
60 using Os isotopes provides improved resolution for changes in seawater chemistry across this
61 boundary section. Combined with data from previous studies this work has two significant
62 outcomes, by providing: (1) an increased geochemical understanding of an important GSSP, thereby
63 also enhancing our understanding of Lower Jurassic stratigraphy in the UK; and (2) a detailed
64 $^{187}Os/^{188}Os$ profile for contemporaneous Jurassic seawater allowing insight into the contributions of
65 the various global inputs into the oceans at this time and therefore providing information regarding
66 ocean connectivity during the Early Jurassic.
67 Currently, the timing of development of oceanic seaways during Pangaean separation is
68 poorly constrained, with estimates that include both the Hettangian and Sinemurian. The Hispanic
69 Corridor, an initially epicontinental, but later fully oceanic seaway, connected the western Tethyan
70 and eastern Pacific oceans along the Central Atlantic rift zone (Smith and Tipper, 1986; Smith et al.,
71 1990; Riccardi, 1991; Hallam and Wignall, 1997; Aberhan, 2001). Formed through separation of the
72 Pangaean supercontinent, this proto-Atlantic seaway resulted from one of the most significant
73 palaeogeographic reorganisations in Earth's history (Smith et al., 1990). Initially developing over
74 rifting continental crust (Smith et al., 1994), this marine corridor signified the tectonic transition
75 from rifting to drifting, prior to the formation of the Atlantic Ocean (Smith et al., 1990). In addition
76 to the profound impact on ocean circulation and equatorial distribution of marine organisms at this
77 time, the marine corridor acted as a filter during its early stages, preferentially allowing passage of
78 on-shore benthic species, whilst acting as an effective barrier for off-shore species (eg. Hallam and
79 Wignall, 1997; Smith et al., 1994; Aberhan, 2001). However, with no direct sedimentological or
80 geophysical evidence, determining the timing for the establishment of the corridor using
81 biogeography has been the subject of continuous debate. As such, the timing of seaway formation is
82 currently imprecise and suggested to have occurred within the Early Jurassic (eg. Damborenea, 2000;
83 Aberhan, 2001).

The $^{187}Os/^{188}Os$ values from the Sinemurian–Pliensbachian GSSP, Robin Hood's Bay, UK, provide evidence for significant low-temperature hydrothermal activity that may have been associated with the formation of the Hispanic Corridor during the breakup of Pangaea. Combined with biogeography and faunal exchange patterns, the Os data herein suggests that connectivity between the Eastern Pacific and Tethyan oceans initiated during the latest Sinemurian. Thus, this study better constrains the timing of establishment of the Hispanic Corridor, previously limited to poorly defined biogeography.

2. Geology of the Sinemurian–Pliensbachian boundary GSSP

Our study focuses on the marine sediments at the Sinemurian–Pliensbachian Global Boundary Stratotype Section and Point (GSSP) at Wine Haven, ~3 km S–SE of Robin Hood's Bay, Yorkshire, UK (Grid ref. NZ9762 0230 eg~~.~~, Hesselbo et al., 2000; Meister et al., 2006; Fig. 1). This Lower Jurassic boundary occurs in the Pyritous Shales of the Redcar Mudstone Formation within the Lias Group (Powell, 1984). It has been the subject of scientific interest for many years, with the earliest reference to the site being by Young and Bird (1822). Exposure at Robin Hood's Bay is optimal, with lower beds exposed by a series of wave-cut platforms. The succession here is also known for its well-preserved ammonite assemblages (eg. Tate and Blake, 1876; Dommergues and Meister, 1992). Using the biostratigraphy, the base of the Pliensbachian Stage can be unambiguously located at the bottom of the *taylori* Subzone of the *Uptonia jamesoni* Zone, marked by the first occurrence of species of the genus *Apoderoceras* (Dean et al., 1961; Hesselbo et al., 2000; Gradstein et al., 2004; Meister et al., 2006).

The age for the base of the Pliensbachian has been defined by the Geological Time Scale (GTS) 2004 as 189.6 ± 1.5 Ma (Gradstein et al., 2004), derived from cycle-scaled linear Sr trends and ammonite occurrences (as noted above; also includes the lowest occurrence of *Bifericeras donovani*; Gradstein et al., 2004). Herein, this age for the Sinemurian–Pliensbachian boundary is used. The

Sinemurian–Pliensbachian boundary is placed very close to the base of Bed 73 (bed classification from Hesselbo and Jenkyns, 1995), ~6 cm above the midline of nodules forming the upper margin of Bed 72 in the Wine Haven section (Hesselbo et al., 2000).

An epicontinental sea, positioned to the west of the deep Tethyan basin (Dera et al., 2009) covered most of Northern Europe, including Britain, during the Mesozoic (Sellwood and Jenkyns, 1975; Fig. 1). Lithological evidence for sea level rise, combined with sedimentological evidence (Smith et al., 1994), indicates that the epicontinental sea during this time was not landlocked but free to circulate with the Tethyan ocean. The open ocean Os isotope composition across the boundary interval should therefore be echoed in the sampled sediments. Analysis of hydrogenous Re and Os from these samples instils certainty that the calculated initial Os isotope composition ($^{187}Os/^{188}Os_{(i)}$) reflects that of contemporaneous seawater (Cohen et al., 1999).

Over a ~10 m interval, the lithology of the Wine Haven succession gradually progresses from pale siliceous and clay-rich mudrocks with intermittent coarser sand beds in the Upper Sinemurian (*aplanatum* Subzone), to finer and much darker shales with less clay ~1.5 m above the boundary in the Lower Pliensbachian (*taylori* Subzone; Meister et al., 2006; Hesselbo and Jenkyns, 1995, 1998; this study). These facies changes indicate an overall relative increase in sea level of at least regional, but possibly global extent (Sellwood, 1972; Hallam, 1981; Hesselbo and Jenkyns 1995, 1998; Hesselbo et al., 2000; Meister et al., 2006).

Nodular beds of concretionary siderite (~10 cm in thickness) of both laterally continuous (Beds 70 and 72) and semi-continuous extent (Bed 74 and within Bed 71) are present throughout the Wine Haven section (Sellwood, 1972; Meister et al., 2006; this study). The origin of these nodules is uncertain, although they are suggested to represent non- or slow depositional phases based on their unique association with fauna found in life-position (Sellwood, 1972).

Sedimentation rate across the Sinemurian–Pliensbachian boundary has been approximated here by taking ~64 Ma as the duration for the Jurassic period (Gradstein et al., 2004) and using mean thicknesses of ammonite zonal subdivisions estimated by Hallam and Sellwood (1976). This provides

a combined thickness for the Sinemurian and Pliensbachian of ~278 m, ~23 % of the total for the Jurassic. By disregarding the uncertain effects of compaction (Hallam and Sellwood, 1976), a steady sedimentation rate during this interval has been calculated at ~1.9 cm/Ka, in turn suggesting that the interval sampled by this study (~6 m) spans ~320 Ka.

Although the $^{87}Sr/^{86}Sr$ profile (Hesselbo et al., 2000) shows a systematic decrease up-section (~0.707487 to 0.707395 over a 10 m interval), a lack of any abrupt changes in the $^{87}Sr/^{86}Sr$ ratio indicates that sedimentation was continuous (Jones et al., 1994; Hesselbo et al., 2000; Meister et al., 2006). At the boundary level, a drop in $^{87}Sr/^{86}Sr$ value from ~0.707433 to 0.707418 (Hesselbo et al., 2000) could allow the possibility of minor slowing or hiatus in sediment deposition (Hesselbo et al., 2000; Meister et al., 2006). However, replicate analyses of belemnites from 1–4 cm above the boundary give an average $^{87}Sr/^{86}Sr$ value of 0.707422 ± 0.000012, well within uncertainty of the ratio recorded for the boundary (0.707425 ± 0.000004) (Hesselbo et al., 2000), suggesting a slowing rather than break in deposition (Hesselbo et al., 2000; Meister et al., 2006). Further evidence for continuous deposition is supported by a lack of lithological unconformities (Meister et al., 2006; this study).

3. Analytical methodology

3.1 Sampling

A set of 32 samples (SP7-09 to SP39-09) were collected from the Pyritous Shales Member of the Redcar Mudstone Formation, along a 6 m vertical section bracketing the Sinemurian–Pliensbachian boundary (sample SP22-09) at Robin Hood's Bay (Fig. 2). Sampling occurred at a consistent interval of ~20 cm for 3 m above and 3 m below the boundary from Beds 69–75 except within Bed 72, where a smaller sampling interval of ~15 cm was used (Fig. 2). Based on our approximation above for the duration of sedimentation across this section, sampling at ~20 cm intervals allowed us to capture an estimated resolution of ~11 Ka per sample.

In preparation for geochemical analyses, the samples were cut and polished to expose fresh surfaces, and were then powdered in a Zr disc.

3.2 Re-Os analysis

Rhenium and osmium analyses of Robin Hood's Bay whole-rock powders were conducted at the Japan Agency for Marine-Earth Science and Technology (JAMSTEC) as part of the JSPS Summer Fellowship Program 2010, following the CrO_3-H_2SO_4 procedure outlined by Selby and Creaser (2003). This digestion technique minimises removal of Re and Os from the non-hydrogenous (detrital) component of the sample, allowing analysis and evaluation of the hydrogenous fraction (Selby and Creaser, 2003). Sample powders of known quantities (500 mg for samples with >50 ppb Re or 1g for samples with <50 ppb Re) were digested with a measured amount of ^{185}Re and ^{190}Os spike solution, in 8 ml of CrO_3-H_2SO_4 solution in Carius tubes at 240 ^{o}C for 48 hrs. After cooling, Os was removed and purified from the solution by solvent extraction and micro-distillation.

Following Os removal, the remaining solution was prepared for anion exchange chromatography to purify the Re fraction. To reduce Cr^{6+} to Cr^{3+}, necessary to avoid complications during chromatography (Selby and Creaser, 2003), 1 ml of the remaining solution was removed and reduced drop by drop (due to the violent exothermic reaction) using 3 ml of ethanol (gradual addition of ethanol to the sample solution is advised to avoid loss of sample during the reduction reaction). Once reduced, the solution was evaporated to dryness on a hotplate at ~80^{o}C.

The dried Re fraction was taken up in a 10 ml 0.5 N HCl loading solution, before being purified by a two-stage HCl-HNO_3 anion chromatography procedure. The purified Re and Os was loaded onto Ni and Pt filaments, respectively and the Re and Os isotope ratios were measured using NTIMS (Creaser et al., 1991; Völkening et al., 1991) using Faraday collectors and the SEM, respectively. The initial Os isotope composition ($^{187}Os/^{188}Os_{(i)}$) was calculated using an independently assumed sample age of ~189.6 Ma (Gradstein et al., 2004) and $\lambda\ ^{187}Re = 1.666 \times 10^{-11}\ a^{-1}$ (Smoliar et al., 1996). During this study total procedural blanks were 14.1 ± 0.2 pg and 3.56 ± 0.52 pg (1σ S.D., n

= 2) for Re and Os, respectively, with an average $^{187}Os/^{188}Os$ value of 0.19 ± 0.005 (n = 2). Uncertainties presented in Table 1 include full error propagation of uncertainties in Re and Os mass spectrometer measurements, blank abundances and isotopic compositions, spike calibrations and reproducibility of standard Re and Os isotopic values.

4. Results

4.1 Re and Os abundance

The Re and Os abundances define a large range of values, from ~1.5–117 and ~0.12–1.9 ppb, respectively (Table 1). These values are much greater than those of average continental crust: 0.39 ppb (Re) and 0.05 ppb (Os) (Sun et al., 2003 and references therein). Both Re and Os abundances show an overall increase up-section that becomes more pronounced following the Sinemurian–Pliensbachian boundary.

4.2 Re-Os geochronology

In order to conduct Re-Os geochronology, the targeted samples should fulfil three criteria. Each sample must possess a similar initial Os isotope composition ($^{187}Os/^{188}Os_{(i)}$) together with variable $^{187}Re/^{188}Os$ ratios, and have experienced no disturbance to the isotope system since the time of formation (Cohen et al., 1999). The Robin Hood's Bay section shows no evidence of post-depositional disturbance, e.g., no veining is evident and the section is thermally immature. Similar Jurassic sections have been utilised for Re-Os geochronology (Cohen et al., 1999).

For the Robin Hood Bay section the $^{187}Re/^{188}Os$ and $^{187}Os/^{188}Os$ ratios vary from ~25–443 and ~0.3–1.6, respectively. Both $^{187}Re/^{188}Os$ and $^{187}Os/^{188}Os$ ratios decrease between 2.8 to 0.9 m below the Sinemurian–Pliensbachian boundary ($^{187}Re/^{188}Os$, ~195–20; $^{187}Os/^{188}Os$, ~1–0.3), before systematically increasing across the boundary into the lowermost Pliensbachian. Although all the $^{187}Re/^{188}Os$ and $^{187}Os/^{188}Os$ ratios positively correlated ($R^2 = 0.95$), the Re-Os data yield model 3 age

of 179 ± 16 Ma (2σ, n = 32, MSWD = 473; Fig. 4a). Although within uncertainty of the calculated age for the Sinemurian–Pliensbachian boundary (189.6 ± 1.5 Ma; Gradstein et al., 2004), the uncertainty is large (~9 %) and is accompanied by an extremely large MSWD, which indicates significant scatter of the data about the isochron that relates to more than analytical uncertainty. We suggest that this scatter relates to the sample set possessing variable initial $^{187}Os/^{188}Os$ values. The calculated initial $^{187}Os/^{188}Os$ ($^{187}Os/^{188}Os_{(i)}$ at 189.6 Ma; Gradstein et al., 2004) values for this Sinemurian–Pliensbachian section are variable, but consistently unradiogenic for all samples, ranging from ~0.20–0.48. Overall, with exceptions at 1.1 m below the boundary and at the boundary itself (sample SP22-09, $^{187}Os/^{188}Os_{(i)}$ = ~0.48 and SP17-09 = ~0.44, respectively; Fig. 3; 4b), the $^{187}Os/^{188}Os_{(i)}$ values become progressively less radiogenic up-section.

If we consider samples with similar $^{187}Os/^{188}Os_{(i)}$ values (~0.20–0.30) regression of the Re-Os data produces a model 3 age of 183.4 ± 3.3 Ma (2σ, n = 17, MSWD = 20; Fig. 4c). This age is outside of uncertainty of that given by Gradstein et al. (2004). Regression of Re-Os data for the top four stratigraphic organic-rich samples in the section (SP34-09, SP35-09, SP36-09 and SP37-09) provides a model 1 age of 194 ± 4.8 Ma (2σ, n = 4, MSWD = 0.04; Fig. 4d). These samples are ideally suited to Re-Os geochronology because they possess extremely similar initial $^{187}Os/^{188}Os$ compositions (~0.20–0.22) and variable $^{187}Re/^{188}Os$ ratios (~268–443). As such, the model age is within uncertainty of that given by Gradstein et al. (2004). Although the Robin Hood bay section is not ideally suited for Re-Os geochronology, the positive correlation of $^{187}Re/^{188}Os$ with $^{187}Os/^{188}Os$ that yields dates that are in agreement with the Geological Time Scale 2004 (Gradstein et al., 2004), suggests that the Re-Os systematics have not been disturbed and that calculated initial $^{187}Os/^{188}Os$ values can be used to discuss Early Jurassic ocean chemistry.

5. Discussion

The Jurassic was a dynamic period that hosted major geological events of Earth's history; notably the full-scale tectonic plate reorganisation associated with the break-up of Pangaea. Ocean chemistry was therefore subject to fluctuations as the balance of inputs changed, and as such the seawater Os isotope composition was highly variable. In order to look critically at the data herein and to determine the potential source of the Os isotope signal observed across the Sinemurian–Pliensbachian boundary, there needs to be an understanding of the background seawater Os isotope composition at this time. However, at present no studies conclusively document background seawater Os for the Early Jurassic. The first estimation of stable, steady-state $^{187}Os/^{188}Os$ values for the Sinemurian is proposed to be ~ 0.47 (Kuroda et al., 2010). The sampled section (Triassic–Jurassic chert succession from Kurusu, Japan; Kuroda et al., 2010) was positioned to the east of the separating supercontinent, in an intra-ocean setting. The recorded Os isotope composition would therefore not have been directly affected by nearby continental flux, and would have been a good representation of open ocean chemistry at this time. For this investigation, we will assume that this value represents the best estimation of background seawater Os isotope composition at the Sinemurian–Pliensbachian transition.

5.1 Origin of the Sinemurian–Pliensbachian seawater Os isotope composition

The Os data from Robin Hoods Bay show that the calculated seawater initial $^{187}Os/^{188}Os$ value becomes progressively more unradiogenic from the latest Sinemurian into the Pliensbachian. Although there is some fluctuation, this trend to unradiogenic values can be broadly separated into three groups, with average $^{187}Os/^{188}Os_{(i)}$ values of ~0.38, 0.28 and 0.21 (Fig. 3). These results indicate that there was a marked and progressive increase of unradiogenic Os input into the global ocean during the transition from the Sinemurian to the Pliensbachian.

A peak towards a relatively radiogenic $^{187}Os/^{188}Os$ value of 0.48 is coincident with the boundary. This is also matched by an increase in the $^{187}Re/^{188}Os$ ratio (from ~31 to 100) and a

decrease in ^{192}Os (from ~208 to 102 ppb). Assuming a background seawater Os isotope composition of ~0.47 (Kuroda et al., 2010), this peak may reflect a period of hiatus in the input of unradiogenic Os to the oceans.

There are three major inputs of Os that directly control the seawater $^{187}Os/^{188}Os$ value: (1) radiogenic input from weathering of continental crust; (2) unradiogenic contribution from meteorites; (3) an unradiogenic signal from igneous and hydrothermal activity (eg. Peucker-Ehrenbrink and Ravizza, 2000).

5.1.1 Why is the signal not induced by continental weathering?

The gradual trend towards unradiogenic Os isotope values observed in this study indicates that continental weathering is unlikely to be the cause of the Os isotopic signal shown over Sinemurian–Pliensbachian boundary. Belemnite oxygen stable isotope data displays a marked increase of ~1 ‰ over 10 m across the boundary (Hesselbo et al., 2000; Fig. 3). This 1 ‰ change is equivalent to a substantial temperature decrease of ~5^{o}C (Hesselbo et al., 2000; Meister et al., 2006). Such considerable lowering of temperature, coupled with evidence for low mean land relief and absence of ice sheets during the Early Jurassic (Golonka et al., 1994), would favour reduced rates of regional and global continental weathering.

The Os isotope signal resulting from continental weathering is also significantly more radiogenic ($^{187}Os/^{188}Os$ = ~1.4; Peucker-Ehrenbrink and Jahn, 2001) than that observed in this study. This indicates that the seawater Os isotope composition was dominated by an unradiogenic source that outweighed the input of radiogenic Os from continental weathering. It is extremely difficult to constrain the exact continental $^{187}Os/^{188}Os$ input to the oceans during the Early Jurassic. However, following Cohen et al. (1999), we can attempt to quantify the approximate contribution of crustal Os into the ocean. Assuming an average $^{187}Os/^{188}Os$ value of ~1.4 for weathering of ancient continental crust (Peucker-Ehrenbrink and Jahn, 2001), and a $^{187}Os/^{188}Os$ value of ~0.13 for an unradiogenic mantle-derived source (Allègre and Luck, 1980; Esser and Turekian, 1993; Sharma et al., 1997;

Levasseur et al., 1998), an input of crustal-sourced Os of 5–22 % is required to obtain seawater $^{187}Os/^{188}Os$ ratios of ~0.44–0.20, respectively. This is small in contrast to the present-day radiogenic contribution to the oceans from the continental crust, of between ~ 70 and 80 % (Peucker-Ehrenbrink, 1996; Sharma et al. 1997), respectively. Given the geographical location of Robin Hood's Bay in close-proximity to continental landmasses (Fig. 5), and the absence of ice sheets, there would almost certainly be radiogenic continental input regardless of land-relief and climate. Further, although challenging to quantify, the epicontinental setting would mean increased sensitivity to continental input. There is no evidence for the weathering of unradiogenic lithologies, e.g., mafic and ultramafic units, thus the decrease in seawater $^{187}Os/^{188}Os$ composition during the earliest Pliensbachian therefore indicates that input of Os into the ocean at this time was dominated by an unradiogenic source, not accounted for by the continental weathering flux.

5.1.2 Why is the unradiogenic Os not from an extraterrestrial source?

Extraterrestrial and mantle-derived influxes are the dominant unradiogenic sources of Os to the global oceans. The calculated $^{187}Os/^{188}Os$ values of these sources (~0.13) are indistinguishable (Allègre and Luck, 1980; Esser and Turekian, 1993; Sharma et al., 1997; Levasseur et al., 1998). It is therefore necessary to examine the structure of the Os isotope profiles from each source to determine which was responsible for the declining unradiogenic Os signal into the Pliensbachian.

Fluctuations in the seawater Os isotope record during the Cenozoic were not induced by extraterrestrial Os influx to the oceans, as the cosmic Os flux was continuous relative to the variable ocean Os record (with the exception of the K–T boundary; Peucker-Ehrenbrink and Ravizza, 2000). Although the extraterrestrial flux to Earth during the Jurassic is poorly constrained, the possibility of meteorite impact at the Sinemurian–Pliensbachian boundary does not reconcile the gradual decline in $^{187}Os/^{188}Os$ ratios. Following an impact, the Os isotope system should recover quickly due to the relatively short seawater residence time of Os (Peucker-Ehrenbrink and Ravizza, 2000). Therefore, although impacts have been documented ~5–20 Ma prior to the Triassic – Jurassic boundary (Hallam

and Wignall, 1997), it would be unlikely to find evidence of meteoritic unradiogenic Os during the Pliensbachian. This is further supported by a study of the Os isotope excursion due to meteorite impact across the K–T boundary (Ravizza and Peucker-Ehrenbrink, 2003), that shows relatively rapid recovery of the Os isotope system to a steady state following impact ($^{187}Os/^{188}Os$ value increases from ~0.16 to 0.40 in a maximum of ~200 Ka).

5.1.3 Unradiogenic Os from a mantle-derived source

The unradiogenic $^{187}Os/^{188}Os$ values are therefore most likely to be mantle-derived. Unlike the other potential sources of oceanic Os discussed above, increased input from a mantle source at the time of the Sinemurian–Pliensbachian boundary can explain the observed isotope profiles.

Rifting of the Pangaean Supercontinent began during the latest Triassic (Marzoli et al., 1999; Hames et al., 2000). The initial stages of continental break-up were focused along the 6000 km lineament that would eventually form the continental margins of the Central North Atlantic Ocean (Hames et al., 2000). Consequently, there is evidence for substantial magmatism during the Late Triassic–Early Jurassic (Marzoli et al., 1999; Hames et al., 2000), defined by extensive continental basalts in North America, Europe, Africa and South America (Wilson, 1997; Marzoli et al., 1999). This formed what is termed as the Central Atlantic Magmatic Province (CAMP). The scale of the CAMP has been postulated to exceed that of the Karoo-Ferrar, the Deccan Traps and the Siberian continental flood basalt provinces (Hames et al., 2000), with a total areal extent and volume of at least 7×10^6 Km^2 and 2×10^6 km^3, respectively (Marzoli et al., 1999; Hames et al., 2000).

High-precision $^{40}Ar/^{39}Ar$ geochronology of the oldest CAMP volcanic rocks, indicate that emplacement occurred during the transition from Late Triassic to Early Jurassic (ca. 200 Ma) with a brief duration of ~ < 2 Ma (Marzoli et al., 1999; Hames et al., 2000). A volcanic event of this magnitude, considering both its sizeable magmatic and hydrothermal outputs, would have had a considerable impact on ocean chemistry, regardless of its exceptionally brief duration (Ravizza and Peucker-Ehrenbrink, 2003). This has been documented by several Os isotope studies of seawater at

the Triassic–Jurassic boundary and during the Hettangian (Cohen et al., 1999; Cohen and Coe, 2002; Cohen, 2004). Prior to and immediately following the Triassic–Jurassic boundary, there was a significant unradiogenic contribution of Os to the oceans that persisted into the Hettangian (Cohen et al., 1999; Cohen and Coe, 2002; Cohen, 2004). This has been attributed to seawater interaction and alteration of recently emplaced CAMP lavas, together with enhanced hydrothermal activity (Cohen et al., 1999; Cohen and Coe, 2002; Cohen, 2004). High chemical weathering rates of juvenile basalts (Louvat and Allègre, 1997) characteristically promote relatively rapid release of unradiogenic Os, which can be seen in the Triassic–Jurassic and Hettangian sample suites (Cohen et al., 1999; Cohen and Coe, 2002; Cohen, 2004). The seawater Os isotopic composition then becomes increasingly unradiogenic across the Sinemurian–Pliensbachian boundary, to $^{187}Os/^{188}Os$ ratios of ~0.20. Using estimates for Early Jurassic stage durations from Gradstein et al. (2004), this boundary occurred ~ 10 Ma after the Triassic–Jurassic boundary and at least ~8 Ma after emplacement of CAMP. Further, the total duration of weathering of CAMP basalts is estimated at ~3.5 Ma (Cohen and Coe, 2007), producing a seawater $^{187}Os/^{188}Os$ value of ~0.30. It is therefore difficult to reconcile the observed Sinemurian–Pliensbachian seawater Os isotope composition with the CAMP emplacement event (ca. 200 Ma) or weathering of the continental flood basalts, given a date for the Sinemurian–Pliensbachian stage boundary of 189.6 ± 1.5 Ma (Gradstein et al., 2004).

However, when considering palaeogeographic and biogeographic evidence, it is possible to determine a mantle-derived origin for the unradiogenic seawater Os isotope composition that does not rely on emplacement of CAMP lavas. Hydrothermal activity would have been prevalent in this tectonic setting, and low temperature hydrothermal fluids have a characteristically unradiogenic Os isotope composition of ~0.12 (Cohen et al., 1999; Sharma et al., 2000).

5.2 Os isotope evidence for oceanic connectivity via the 'Hispanic Corridor' during the Early Pliensbachian

The separation of Pangaea and onset of a global sea level rise established a number of epeiric seaways, including the Hispanic Corridor (Aberhan, 2001). This initially epicontinental, but later fully oceanic seaway was established along the Central Atlantic rift zone, between the areas of North America, South America and Africa (Smith and Tipper, 1986), eventually connecting the western Tethyan and eastern Pacific oceans (eg. Smith and Tipper, 1986; Smith et al., 1990; Riccardi, 1991; Aberhan, 2001; Fig. 5).

No connectivity existed between these oceans during the Hettangian or Sinemurian, providing an effective barrier to oceanic circulation and thus to faunal exchange (eg. Smith and Tipper, 1986; Riccardi, 1991; Aberhan, 2001). In addition, biogeographic and sedimentological evidence indicates that an oceanic corridor did not develop before the Middle Jurassic (Aberhan, 2001). Whilst some studies, based on benthic faunas, postulate an opening time for the corridor of Late Triassic (Sandy and Stanley, 1993) and early Hettangian (Sha, 2002), substantial evidence for sudden low levels of faunal exchange between the eastern Pacific and western Tethyan oceans exists in the earliest Pliensbachian (Damborenea and Manceñido, 1979; Smith and Tipper, 1986; Smith et al., 1990). This suggests establishment of the Hispanic Corridor as a shallow but continuous seaway by the start of the Pliensbachian. Schootbrugge et al. (2005) also suggest that short bursts in the diversification of dinoflagellates during the latest Sinemurian are consistent with the opening of this seaway.

The decline of seawater $^{187}Os/^{188}Os$ ratios and the rise in sea level evident across the Sinemurian–Pliensbachian boundary section at Wine Haven, are therefore coincident with the onset of flooding of the Hispanic Corridor. Furthermore, this study suggests that the isotopic signals observed at the boundary reflect increasing hydrothermal activity associated with the opening of the Hispanic Corridor.

394 The Hispanic Corridor developed across rifting continental crust (Smith et al., 1994), with
395 significant crustal stretching and attenuation occurring before creation of the oceanic strait (Hallam
396 and Wignall, 1997). Growing evidence also indicates that substantial off-axis hydrothermal venting
397 may occur in cooler crustal regions away from the immediate rift zone, driven by exothermic
398 reactions between seawater and mantle-derived rocks (Kelley et al., 2001). This is evident at the
399 Mid-Atlantic and Juan de Fuca ridges, respectively (Kelley et al., 2001; Sharma et al., 2000),. Off-axis
400 fluids are typically cool (~40–75^{o}C) with high Os concentrations (~500 femtomol/kg) and
401 unradiogenic $^{187}Os/^{188}Os$ ratios of ~0.12 (Sharma et al., 2000). Mantle-derived material (basalt) was
402 prevalent in this Central Atlantic region (eg. Wilson, 1997; Marzoli et al., 1999), allowing seawater-
403 rock interaction to ensue following the initial flooding event. This would have driven extensive low-
404 temperature hydrothermal fluid circulation, promoting an increase in the release of unradiogenic Os
405 into the seawater (Sharma et al., 2000).
406
407
408 **6. Conclusions**

409 The Sinemurian–Pliensbachian boundary GSSP at Robin Hood's Bay, UK, has the potential to
410 provide a significantly increased understanding of seawater chemistry during the Early Jurassic.
411 Further, understanding changes in ocean chemistry during this time has the potential to yield
412 valuable insight into ocean connectivity during Pangaean separation.
413 Seawater during the Sinemurian–Pliensbachian transition became dominated by an
414 unradiogenic $^{187}Os/^{188}Os$ signal that is not resolvable by influxes from continental weathering or
415 meteorite impact. The break-up of Pangaea was of fundamental importance to this observed
416 isotopic trend, and a mantle-derived source favours the constructed Os isotope profile.
417 The Triassic–Jurassic boundary marks the onset of volcanism in the Central Atlantic
418 Magmatic Province, directly associated with Pangaean fragmentation. Following this there is strong
419 taxonomic evidence for sudden, albeit restricted levels, of faunal exchange between the western

Tethyan and eastern Pacific oceans in the latest Sinemurian and the start of the Pliensbachian, via the Hispanic Corridor (defining the rift zone between North America, South America and Africa). This stage boundary therefore marks the initial flooding event of the Hispanic Corridor that also corresponds to an on-going global sea level rise. Seawater inundation would have initiated seawater interaction with, and circulation into, deep crustal fissures associated with rifting in this region, thus driving extensive low-temperature hydrothermal activity. Such low-temperature hydrothermal fluids are characterised by unradiogenic $^{187}Os/^{188}Os$ ratios of ~0.12 (Sharma et al., 2000; Kelley et al., 2001). It is therefore possible that the unradiogenic $^{187}Os/^{188}Os$ signal observed across the Sinemurian–Pliensbachian boundary marks the onset of hydrothermal activity associated with formation of the Hispanic Corridor.

Acknowledgments

This research was supported through the JSPS Summer Fellowship Program, hosted by the Japan Agency for Marine-Earth Science and Technology (JAMSTEC) and a NERC PhD studentship to SJP. Thanks to Katz Suzuki, Ryoko Senda and Akira Ishikawa for their assistance in the laboratory.

Figure captions

Fig. 1. Map showing the European epicontinental sea and the geographical relationship between the Hispanic Corridor, Tethyan Ocean and Robin Hood's Bay. Modified after Dera et al. (2009). A location map of the Wine Haven section is also provided.

Fig. 2. Graphic log showing the Sinemurian–Pliensbachian boundary GSSP and the relative locations of the samples analysed in this study. Bed number classification taken from Hesselbo and Jenkyns (1995).

Fig. 3. Re-Os isotope stratigraphy across the Sinemurian–Pliensbachian boundary GSSP, UK. Strontium isotope ($^{87}Sr/^{86}Sr$) from Jones et al. (1994) and Hesselbo et al. (2000), and $\delta^{18}O$ data from Hesselbo et al. (2000). Grey dashed line, A, reflects the three groups of $^{187}Os/^{188}Os_{(i)}$ values for seawater across the Sinemurian–Pliensbachian boundary (~0.38, 0.28 and 0.21). Black dashed line, B[1], represents the first estimation of stable steady-state $^{187}Os/^{188}Os$ values for Early Jurassic seawater (~0.47; Kuroda et al., 2010). Bed number classification taken from Hesselbo and Jenkyns (1995).

Fig. 4. a) Rhenium-osmium isochron for all Robin Hood's Bay samples (n = 32); **b)** Histogram showing the variability of the initial $^{187}Os/^{188}Os$ ratio in the Robin Hood's Bay sediments, calculated at 189.6 Ma; **c)** All Robin Hood's Bay samples with initial $^{187}Os/^{188}Os$ ratios between ~0.20 – 0.30 (n = 17); **d)** The four samples at the top of the studied Robin Hood's Bay section, with variable $^{187}Re/^{188}Os$ ratios (~268 – 443) and similar initial $^{187}Os/^{188}Os$ ratios (~0.20 – 0.22).

Fig. 5. Global reconstruction of Pangaea in the Early Jurassic. Map shows the relative locations of the Central Atlantic Magmatic Province (CAMP), the Hispanic Corridor, the Tethyan and Pacific oceans and Robin Hood's Bay. Modified after www.scotese.com.

Table 1. Re and Os isotope data for the Sinemurian–Pliensbachian boundary GSSP, UK.

References

Aberhan, M., 2001. Bivalve palaeobiogeography and the Hispanic Corridor: time of opening and effectiveness of a proto-Atlantic seaway. Palaeogeography, Palaeoclimatology, Palaeoecology 165, 375-394.

Allègre, C.J., Luck, J.-M., 1980. Osmium isotopes as petrogenetic and geological tracers. Earth and Planetary Science Letters 48, 148-154.

Cohen, A.S., 2004. The rhenium-osmium isotope system: applications to geochronological and palaeoenvironmental problems. Journal of the Geological Society of London 161, 729-734.

Cohen, A.S., Coe, A.L., 2002. New geochemical evidence for the onset of volcanism in the central Atlantic magmatic province and environmental change at the Triassic–Jurassic boundary. Geology 30, 267-270.

Cohen, A.S., Coe, A.L., 2007. The impact of the Central Atlantic Magmatic Province on climate and on the Sr- and Os-isotope evolution of seawater. Palaeogeography, Palaeoclimatology, Palaeoecology 244, 374-390.

Cohen, A.S., Coe, A.L., Bartlett, J.M., Hawkesworth, C.J., 1999. Precise Re-Os ages of organic-rich mudrocks and the Os isotope composition of Jurassic seawater. Earth and Planetary Science Letters 167, 159-173.

Creaser, R.A., Papanastassiou, D.A., Wasserburg, G.J., 1991. Negative thermal ion mass spectrometry of osmium, rhenium and iridium. Geochimica et Cosmochimica Acta 55, 397-401.

Damborenea, S.E., 2000. Hispanic Corridor: Its evolution and biogeography of bivalve molluscs. In: Hall, R., Smith, P.L. (Eds.), Advances in Jurassic Research 2000. Proceedings of the Fifth International Symposium on the Jurassic System, Trans Tech, Switzerland. GeoResearch Forum, pp. 369-380.

Damborenea, S.E., Manceñido, M.O., 1979. On the palaeogeographical distribution of the pectinid genus Weyla (Bivalvia, lower Jurassic). Palaeogeography, Palaeoclimatology, Palaeoecology 27, 85-102.

Dean, W.T., Donovan, D.T., Howarth, M.K., 1961. The Liassic ammonite Zones and Subzones of the North West European Province. Bulletin of the Natural History Museum 4, 435-505.

Dera, G., Pucéat, E., Pellenard, P., Neige, P., Delsate, D., Joachimski, M.M., Reisberg, L., Martinez, M., 2009. Water mass exchange and variations in seawater temperature in the NW Tethys during the Early Jurassic: Evidence from neodymium and oxygen isotopes of fish teeth and belemnites. Earth and Planetary Science Letters 286, 198-207.

501 Dommergues, J.-L., Meister, C., 1992. Late Sinemurian and Early Carixian ammonites in Europe with
502 cladistic analysis of sutural characteristics. Neues Jahrbuch fur Geologie and Palaontologie
503 Abhandlungen 185, 211-237.
504 Esser, B.K., Turekian, K.K., 1993. The osmium isotopic composition of the continental crust.
505 Geochimica et Cosmochimica Acta 57, 3093-3104.
506 Golonka, J., Ross, M.I., Scotese, C.R., 1994. Phanerozoic paleogeographic and paleoclimatic modeling
507 maps. In: Embry, A.F., Beauchamp, B., Glass, D.J. (Eds.), Pangaea: Global environments and
508 resources. Canadian Society of Petroleum Geologists Memoir 17, 1-47.
509 Gradstein, F.M., Ogg, J.G., Smith, A.G., Bleeker, W., Lourens, L.J., 2004. A new Geologic Time Scale,
510 with special reference to Precambrian and Neogene. Episodes 27, 83-100.
511 Hallam, A., 1981. A revised sea-level cruve for the early Jurassic. Journal of the Geological Society of
512 London 138, 735-743.
513 Hallam, A., Sellwood, B.W., 1976. Middle Mesozoic Sedimentation in Relation to Tectonics in the
514 British Area. Journal of Geology 84, 301-321.
515 Hallam, A., Wignall, P.B., 1997. Mass Extinctions and Their Aftermath. Oxford University Press,
516 Oxford.
517 Hames, W.E., Renne, P.R., Ruppel, C., 2000. New evidence for geologically instantaneous
518 emplacement of earliest Jurassic Central Atlantic Magmatic Province basalts on the North
519 American margin. Geology 28.
520 Hesselbo, S.P., Jenkyns, H.C., 1995. A comparison of the Hettangian to Bajocian successions of
521 Dorset and Yorkshire. In: Taylor, P.D. (Ed.), Field Geology of the British Jurassic. Geological
522 Society of London, pp. 105-150.
523 Hesselbo, S.P., Jenkyns, H.C., 1998. British Lower Jurassic Sequence Stratigraphy. In: De Graciansky,
524 P.C., Hardenbol, J., Jacquin, T., Vail, P.R. (Eds.), Mesozoic and Cenozoic Sequence Stratigraphy
525 of European Basins. Special Publication of the Society for Sedimentary Geology (SEPM) 60, pp.
526 561-581.
527 Hesselbo, S.P., Meister, C., Gröcke, D.R., 2000. A potential global stratotype for the Sinemurian–
528 Pliensbachian boundary (Lower Jurassic), Robin Hood's Bay, UK: ammonite faunas and isotope
529 stratigraphy. Geological Magazine 137, 601-607.
530 Jones, C.E., Jenkyns, H.C., 2001. Seawater strontium isotopes, oceanic anoxic events, and seafloor
531 hydrothermal activity in the Jurassic and Cretaceous. American Journal of Science 301, 112-
532 149.
533 Jones, C.E., Jenkyns, H.C., Hesselbo, S.P., 1994. Strontium isotopes in Early Jurassic seawater.
534 Geochimica et Cosmochimica Acta 58, 1285-1301.

Kelley, D.S., Karson, J.A., Blackman, D.K., Fruh-Green, G.L., Butterfield, D.A., Lilley, M.D., Olson, E.J., Schrenk, M.O., Roe, K.K., Lebon, G.T., Rivizzigno, P., Party, A.-S., 2001. An off-axis hydrothermal vent field near the Mid-Atlantic Ridge at 30°N. Nature 412, 145-149.

Kuroda, J., Hori, R.S., Suzuki, K., Gröcke, D.R., Ohkouchi, N., 2010. Marine osmium isotope record across the Triassic–Jurassic boundary from a Pacific pelagic site. Geology 38, 1095-1098.

Levasseur, S., Birck, J.-L., Allègre, C.J., 1998. Direct Measurement of Femtomoles of Osmium and the $^{187}Os/^{186}Os$ Ratio in Seawater. Science 282, 272-274.

Levasseur, S., Birck, J.L., Allègre, C.J., 1999. The osmium riverine flux and the oceanic mass balance of osmium. Earth and Planetary Science Letters 174, 7-23.

Louvat, P., Allègre, C.J., 1997. Present denudation rates on the island of Réunion determined by river geochemistry: Basalt weathering and mass budget between chemical and mechanical erosions. Geochimica et Cosmochimica Acta 61, 3645-3669.

Marzoli, A., Renne, P.R., Piccirillo, E.M., Ernesto, M., Bellieni, G., De Min, A., 1999. Extensive 200-Million-Year-Old Continental Flood Basalts of the Central Atlantic Magmatic Province. Science 284, 616-618

Meister, C., Aberhan, M., Blau, J., Dommergues, J.-L., Feist-Burkhardt, S., Hailwood, E.A., Hart, M., Hesselbo, S.P., Hounslow, M.W., Hylton, M., Morton, N., Page, K., Price, G.D., 2006. The Global Boundary Stratotype Section and Point (GSSP) for the base of the Pliensbachian Stage (Lower Jurassic), Wine Haven, Yorkshire, UK. Episodes 29, 93-114.

Oxburgh, R., 1998. Variations in the osmium isotope composition of sea water over the past 200,000 years. Earth and Planetary Science Letters 159, 183-191.

Palmer, M.R., Falkner, K.K., Turekian, K.K., Calvert, S.E., 1988. Sources of osmium isotopes in manganese nodules. Geochimica et Cosmochimica Acta 52, 1197-1202.

Peucker-Ehrenbrink, B., 1996. Accretion of extraterrestrial matter during the last 80 million years and its effect on the marine osmium isotope record. Geochimica et Cosmochimica Acta 60, 3187-3196.

Peucker-Ehrenbrink, B., Jahn, B., 2001. Rhenium-osmium isotope systematics and platinum group element concentrations: Loess and the upper continental crust. Geochemistry, Geophysics, Geosystems 2, 1061-1083.

Peucker-Ehrenbrink, B., Ravizza, G., 2000. The marine osmium isotope record. Terra Nova 12, 205-219.

Powell, J.H., 1984. Lithostratigraphical nomenclature of the Lias Group in the Yorkshire Basin. Proceedings of the Yorkshire Geological Society 45, 51-57.

568 Ravizza, G., Martin, C.E., German, C.R., Thompson, G., 1996. Os isotopes as tracers in seafloor
569 hydrothermal systems: metalliferous deposits from the TAG hydrothermal area, 26°N Mid-
570 Atlantic Ridge. Earth and Planetary Science Letters 138, 105-119.
571 Ravizza, G., Peucker-Ehrenbrink, B., 2003. Chemostratigraphic Evidence of Deccan Volcanism from
572 the Marine Osmium Isotope Record. Science 302, 1392-1395.
573 Riccardi, A.C., 1991. Jurassic and Cretaceous marine connections between the Southeast Pacific and
574 Tethys. Palaeogeography, Palaeoclimatology, Palaeoecology 87, 155-189.
575 Sandy, M. R., Stanley, G.D., 1993. Late Triassic brachiopods from the Luning Formation, Nevada, and
576 their paleogeographical significance. Palaeontology 36, 439-480.
577 Schootbrugge, B., Bailey, T.R., Rosenthal, Y., Katz, M.E., Wright, J.D., Miller, K.G., Feist-Burkhardt, S.,
578 Falkowski, P.G., 2005. Early Jurassic climate change and the radiation of organic-walled
579 phytoplankton in the Tethys Ocean. Paleobiology 31, 73-97.
580 Selby, D., Creaser, R.A., 2003. Re-Os geochronology of organic rich sediments: an evaluation of
581 organic matter analysis methods. Chemical Geology 200, 225-240.
582 Sellwood, B.W., Jenkyns, H.C., 1975. Basins and swells and the evolution of an epeiric sea
583 (Pliensbachian-Bajocian of Great Britain). Journal of the Geological Society of London 131,
584 373-388.
585 Sellwood, W., 1972. Regional environmental changes across a Lower Jurassic stage-boundary in
586 Britain. Palaeontology 15, 125-157.
587 Sha, J., 2002. Hispanic Corridor formed as early as Hettangian: On the basis of bivalve fossils. Chinese
588 Science Bulletin 47, 414-417.
589 Sharma, M., Papanastassiou, D.A., Wasserburg, G.J., 1997. The concentration and isotopic
590 composition of osmium in the oceans. Geochimica et Cosmochimica Acta 61, 3287-3299.
591 Sharma, M., Wasserburg, G.J., Hofmann, A.W., Butterfield, D.A., 2000. Osmium isotopes in
592 hydrothermal fluids from the Juan de Fuca Ridge. Earth and Planetary Science Letters 179,
593 139-152.
594 Smith, A.G., Smith, D.G., Funnell, B.M., 1994. Atlas of Mesozoic and Cenozoic Coastlines. Cambridge
595 University Press.
596 Smith, P.L., Tipper, H.W., 1986. Plate Tectonics and Paleobiogeography: Early Jurassic (Pliensbachian)
597 Endemism and Diversity. Palaios 1, 399-412.
598 Smith, P.L., Westermann, G.E.G., Stanley, G.D., Jr., Yancey, T.E., Newton, C.R., 1990.
599 Paleobiogeography of the Ancient Pacific. Science 249, 680-683.
600 Smoliar, M.I., Walker, R.J., Morgan, J.W., 1996. Re-Os Ages of Group IIA, IIIA, IVA, and IVB Iron
601 Meteorites. Science 23, 1099-1102.

602 Sun, W., Bennett, V.C., Eggins, S.M., Kamenetsky, V.S., Arculus, R.J., 2003. Enhanced mantle-to-crust
603 rhenium transfer in undegassed arc magmas. Nature 422, 294-297.
604 Tate, R., Blake, J.F., 1876. The Yorkshire Lias. J. van Voorst, London.
605 Völkening, J., Walczyk, T., G. Heumann, K., 1991. Osmium isotope ratio determinations by negative
606 thermal ionization mass spectrometry. International Journal of Mass Spectrometry and Ion
607 Processes 105, 147-159.
608 Wilson, M., 1997. Thermal evolution of the Central Atlantic passive margins: continental break-up
609 above a Mesozoic super-plume. Journal of the Geological Society of London 154, 491-495.
610 Young, G.M., Bird, J., 1822. A geological survey of the Yorkshire Coast: describing the strata and
611 fossils occurring between the Humber and the Tees, from the German Ocean to the Plain of
612 York. Whitby. 366.
613
614 www.scotese.com (Figure 5: Pangaean reconstruction in the Early Jurassic)

Figure 1

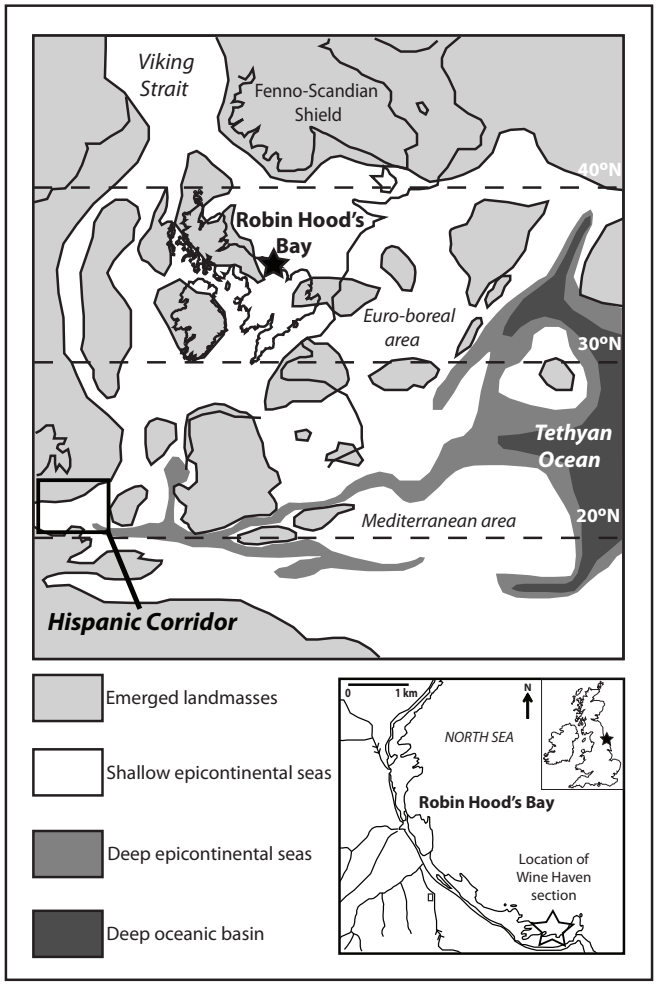
Viking Strait
Fenno-Scandian Shield
40°N
Robin Hood's Bay
Euro-boreal area
30°N
Tethyan Ocean
Mediterranean area
20°N
Hispanic Corridor
Emerged landmasses
Shallow epicontinental seas
Deep epicontinental seas
Deep oceanic basin
0
1 km
N
NORTH SEA
Robin Hood's Bay
Location of Wine Haven section

Figure 2

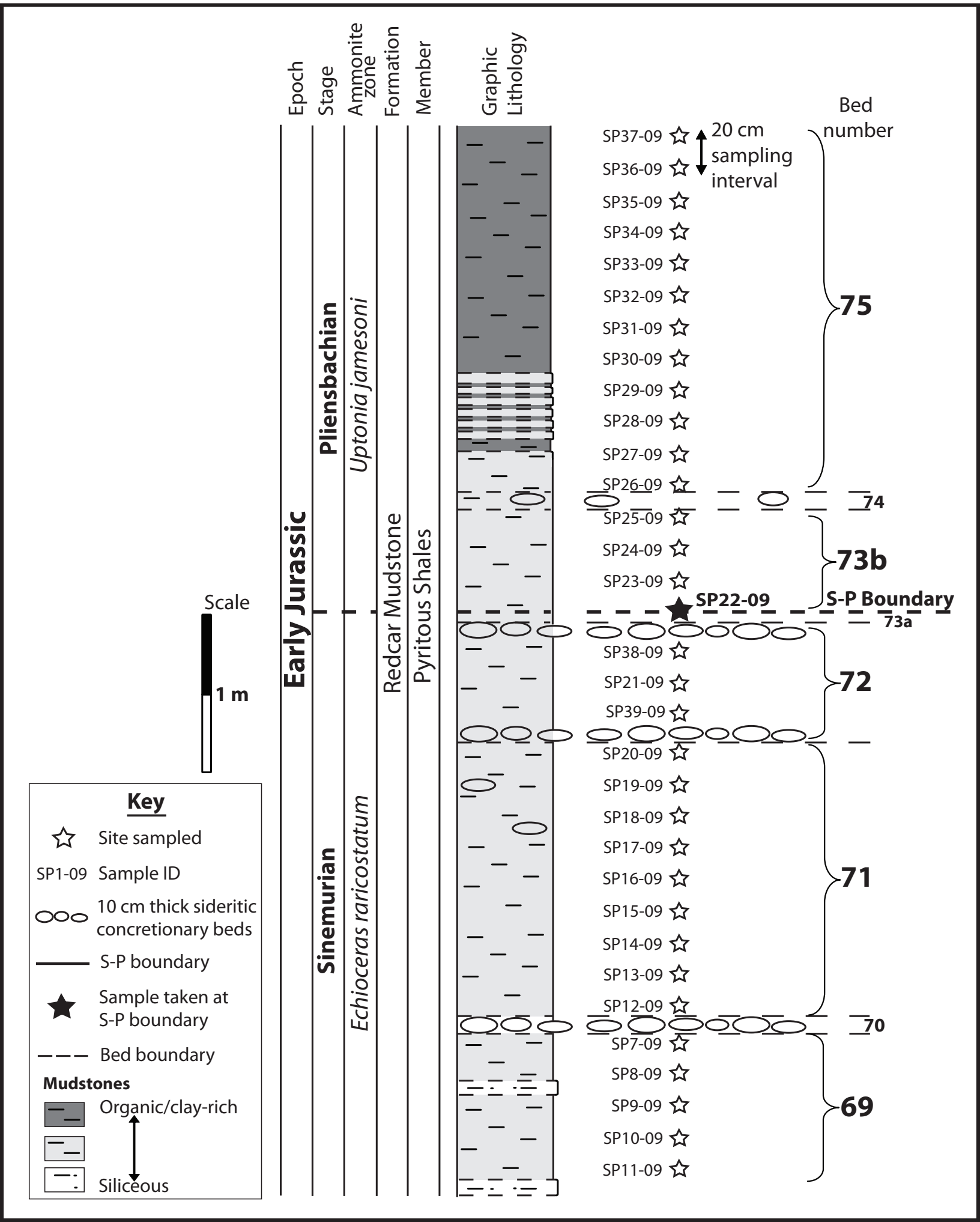
Epoch
Stage
Ammonite zone
Formation
Member
Graphic Lithology
Bed number
Early Jurassic
Pliensbachian
Sinemurian
Uptonia jamesoni
Echioceras raricostatum
Redcar Mudstone
Pyritous Shales
20 cm sampling interval
SP37-09
SP36-09
SP35-09
SP34-09
SP33-09
SP32-09
SP31-09
SP30-09
SP29-09
SP28-09
SP27-09
SP26-09
SP25-09
SP24-09
SP23-09
SP22-09
SP38-09
SP21-09
SP39-09
SP20-09
SP19-09
SP18-09
SP17-09
SP16-09
SP15-09
SP14-09
SP13-09
SP12-09
SP7-09
SP8-09
SP9-09
SP10-09
SP11-09
75
74
73b
S-P Boundary
73a
72
71
70
69
Scale
1 m
Key
Site sampled
SP1-09 Sample ID
10 cm thick sideritic concretionary beds
S-P boundary
Sample taken at S-P boundary
Bed boundary
Mudstones
Organic/clay-rich
Siliceous

Figure 3

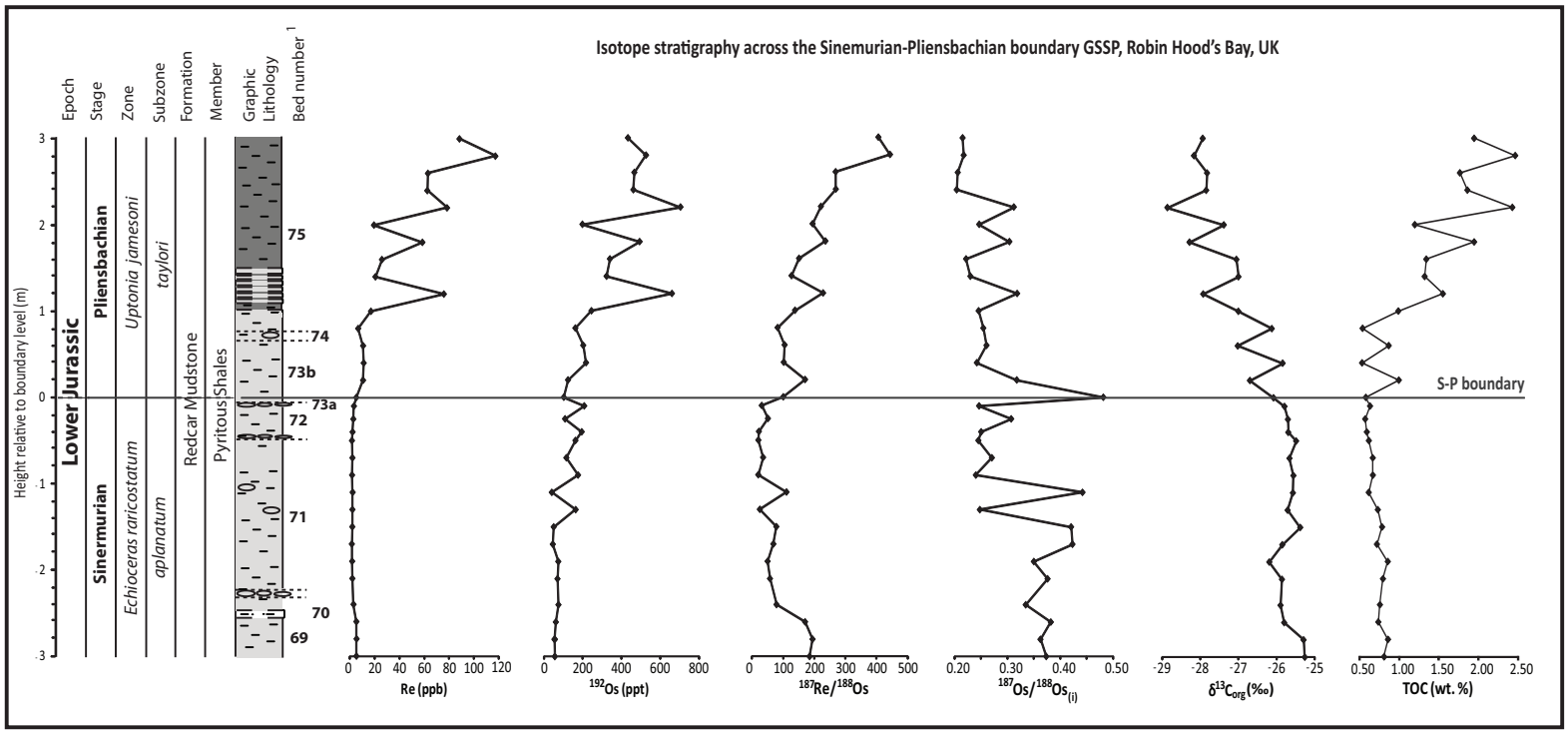
Isotope stratigraphy across the Sinemurian-Pliensbachian boundary GSSP, Robin Hood's Bay, UK
Epoch
Stage
Zone
Subzone
Formation
Member
Graphic Lithology
Bed number
Height relative to boundary level (m)
Lower Jurassic
Sinemurian
Pliensbachian
Echioceras raricostatum
aplanatum
Uptonia jamesoni
taylori
Redcar Mudstone
Pyritous Shales
75
74
73b
73a
72
71
70
69
S-P boundary
Re (ppb)
192Os (ppt)
187Re/188Os
187Os/188Os(i)
δ13Corg (‰)
TOC (wt. %)

Figure 4

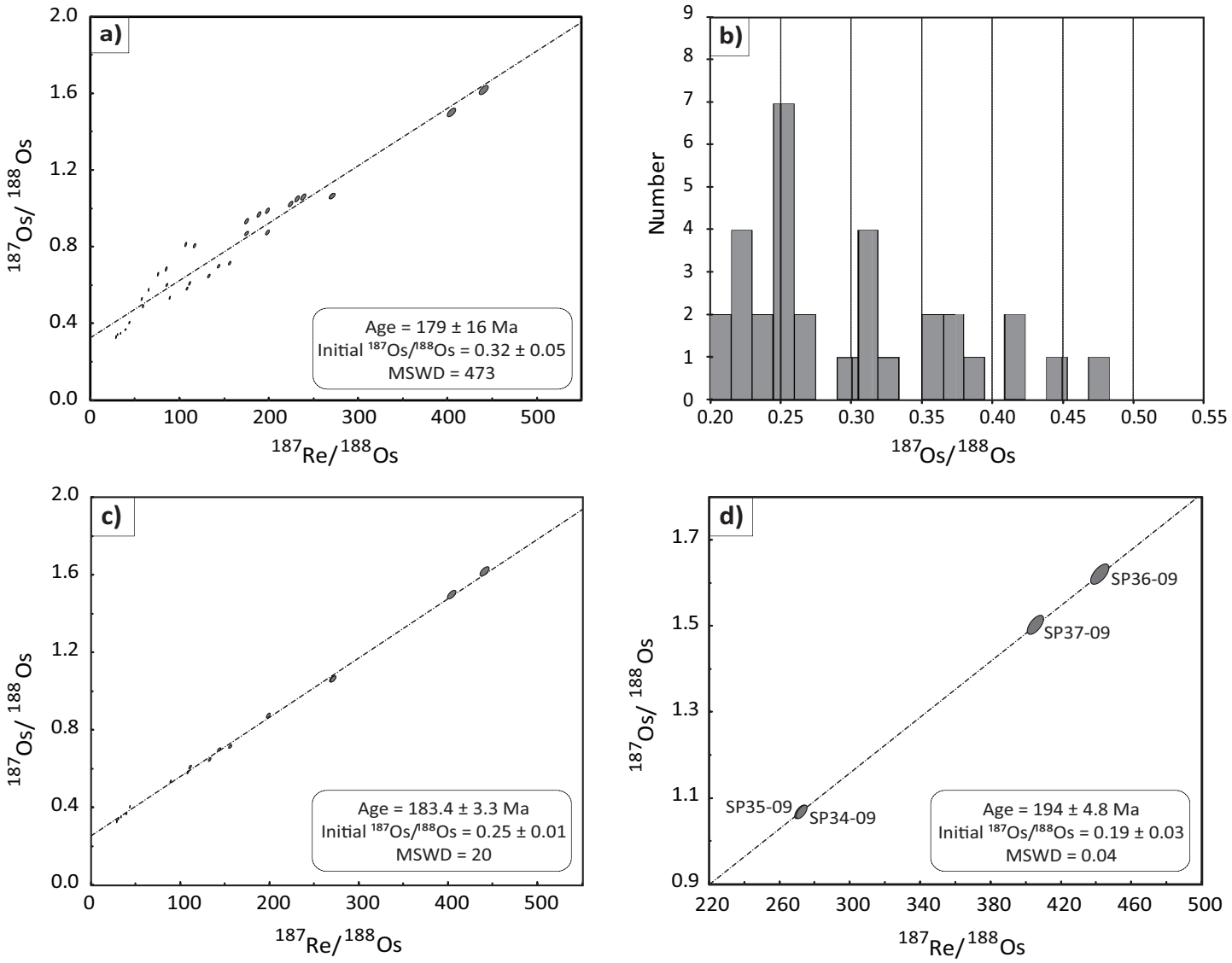
a)
Age = 179 ± 16 Ma
Initial $^{187}Os/^{188}Os$ = 0.32 ± 0.05
MSWD = 473
$^{187}Os/^{188}Os$
$^{187}Re/^{188}Os$
b)
Number
$^{187}Os/^{188}Os$
c)
Age = 183.4 ± 3.3 Ma
Initial $^{187}Os/^{188}Os$ = 0.25 ± 0.01
MSWD = 20
$^{187}Os/^{188}Os$
$^{187}Re/^{188}Os$
d)
SP36-09
SP37-09
SP35-09
SP34-09
Age = 194 ± 4.8 Ma
Initial $^{187}Os/^{188}Os$ = 0.19 ± 0.03
MSWD = 0.04
$^{187}Os/^{188}Os$
$^{187}Re/^{188}Os$

Figure 5

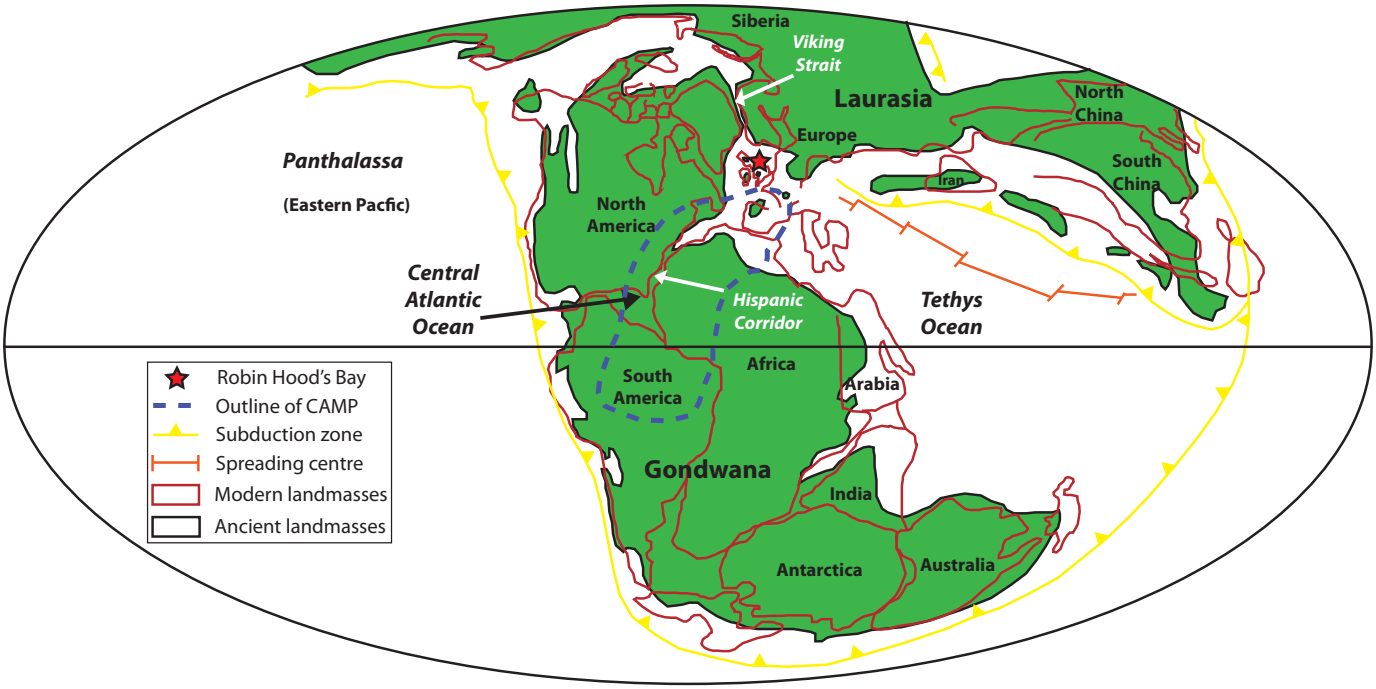
Siberia
Viking Strait
Laurasia
North China
Europe
South China
Iran
Panthalassa
(Eastern Pacfic)
North America
Central Atlantic Ocean
Hispanic Corridor
Tethys Ocean
Africa
Arabia
South America
Gondwana
India
Antarctica
Australia
Robin Hood's Bay
Outline of CAMP
Subduction zone
Spreading centre
Modern landmasses
Ancient landmasses

Table 1

Sample	Distance from S-P boundary (m)	Bed number	Re (ppb)	Os (ppt)	^{192}Os (ppt)	$^{187}Re/^{188}Os$	$^{187}Os/^{188}Os$	Rho [a]	$^{187}Os/^{188}Os_{(i)}$ [b]
SP37-09	3.0	75	88.40 ± 0.39	1237.56 ± 8.93	433.22	405.93 ± 3.96	1.502 ± 0.0184	0.630	0.22
SP36-09	2.8	75	117.36 ± 0.52	1524.48 ± 11.26	526.64	443.32 ± 4.32	1.623 ± 0.0199	0.630	0.22
SP35-09	2.6	75	62.97 ± 0.28	1266.69 ± 8.25	466.35	268.63 ± 2.62	1.058 ± 0.0130	0.629	0.21
SP34-09	2.4	75	62.45 ± 0.28	1253.15 ± 8.16	461.36	269.28 ± 2.63	1.058 ± 0.0130	0.629	0.20
SP33-09	2.2	75	78.38 ± 0.35	1903.42 ± 12.26	704.34	221.37 ± 2.16	1.014 ± 0.0125	0.630	0.31
SP32-09	2.0	75	19.44 ± 0.09	527.43 ± 3.24	198.66	194.69 ± 1.90	0.864 ± 0.0106	0.630	0.25
SP31-09	1.8	75	58.51 ± 0.26	1339.44 ± 8.71	493.48	235.86 ± 2.30	1.052 ± 0.0129	0.629	0.30
SP30-09	1.6	75	25.86 ± 0.12	885.97 ± 5.15	340.30	151.16 ± 1.47	0.701 ± 0.0086	0.628	0.22
SP29-09	1.4	75	20.62 ± 0.09	833.96 ± 4.73	323.00	127.03 ± 1.24	0.633 ± 0.0078	0.629	0.23
SP28-09	1.2	75	75.81 ± 0.34	1790.13 ± 11.60	660.20	228.44 ± 2.23	1.043 ± 0.0128	0.628	0.32
SP27-09	1.0	75	17.02 ± 0.08	636.65 ± 3.68	245.05	138.20 ± 1.35	0.684 ± 0.0084	0.629	0.25
SP26-09	0.8	75	6.71 ± 0.03	412.56 ± 2.23	162.12	82.29 ± 0.81	0.515 ± 0.0063	0.628	0.25
SP25-09	0.6	73b	10.69 ± 0.05	520.99 ± 2.91	202.77	104.85 ± 1.02	0.593 ± 0.0073	0.629	0.26
SP24-09	0.4	73b	11.15 ± 0.05	556.50 ± 3.07	217.32	102.05 ± 1.00	0.566 ± 0.0070	0.629	0.24
SP23-09	0.2	73b	10.65 ± 0.05	329.82 ± 2.03	124.31	170.51 ± 1.67	0.858 ± 0.0106	0.631	0.32
SP22-09	0.0	S-P boundary	5.19 ± 0.02	270.47 ± 1.64	102.65	100.56 ± 0.99	0.801 ± 0.0099	0.629	0.48
SP38-09	-0.1	72	3.28 ± 0.04	518.25 ± 2.57	208.02	31.38 ± 0.44	0.346 ± 0.0043	0.436	0.25
SP21-09	-0.3	72	2.81 ± 0.01	275.83 ± 1.46	109.00	51.30 ± 0.52	0.470 ± 0.0058	0.616	0.31
SP39-09	-0.4	72	2.19 ± 0.01	484.32 ± 2.37	195.01	22.32 ± 0.23	0.321 ± 0.0040	0.606	0.25
SP20-09	-0.5	71	1.68 ± 0.01	403.24 ± 1.96	162.59	20.58 ± 0.21	0.310 ± 0.0038	0.590	0.25
SP19-09	-0.7	71	2.08 ± 0.01	289.80 ± 1.47	115.77	35.73 ± 0.37	0.384 ± 0.0047	0.605	0.27
SP18-09	-0.9	71	1.79 ± 0.01	436.18 ± 2.11	176.00	20.27 ± 0.21	0.305 ± 0.0037	0.595	0.24
SP17-09	-1.1	71	2.27 ± 0.01	107.09 ± 0.66	40.68	110.84 ± 1.17	0.794 ± 0.0101	0.629	0.44
SP16-09	-1.3	71	2.09 ± 0.01	407.07 ± 2.00	163.76	25.33 ± 0.26	0.328 ± 0.0040	0.601	0.25
SP15-09	-1.5	71	1.98 ± 0.01	130.77 ± 0.77	50.43	78.30 ± 0.82	0.669 ± 0.0084	0.615	0.42
SP14-09	-1.7	71	1.58 ± 0.01	118.28 ± 0.69	45.76	68.82 ± 0.75	0.642 ± 0.0081	0.595	0.42
SP13-09	-1.9	71	1.87 ± 0.01	188.64 ± 1.03	74.18	50.21 ± 0.52	0.509 ± 0.0063	0.603	0.35
SP12-09	-2.1	71	2.03 ± 0.01	179.00 ± 1.00	69.96	57.81 ± 0.60	0.560 ± 0.0070	0.609	0.38
SP8-09	-2.3	69	2.97 ± 0.01	192.49 ± 1.08	74.99	78.84 ± 0.80	0.585 ± 0.0073	0.622	0.33
SP9-09	-2.6	69	5.26 ± 0.02	164.12 ± 1.04	61.38	170.52 ± 1.71	0.923 ± 0.0115	0.636	0.38
SP10-09	-2.8	69	5.43 ± 0.02	149.32 ± 0.97	55.48	194.57 ± 1.95	0.980 ± 0.0122	0.638	0.36
SP11-09	-3.0	69	5.29 ± 0.02	152.90 ± 0.98	56.94	184.94 ± 1.86	0.960 ± 0.0120	0.637	0.37

Results presented to 2σ level of uncertainty.

[a] Rho is the associated error correlation (Ludwig, 1980)

[b] The initial $^{187}Os/^{188}Os$ isotope ratio calculated at 189.6 Ma

Ages calculated using the $\lambda\,^{187}Re = 1.666 \times 10^{-11}\ yr^{-1}$